Table 1 Patient characteristics based on the presence of CADM or anti-MDA-5 antibodies

			CADM			α-MDA-5-positive		
Years of sera collection	Total number of DM patients (M:F)	Mean age at onset (range)	Number (%) of patients (M:F)	*P* value*	Mean age at onset (range)	Number (%) of patients (M:F)	*P* value**	Mean age at onset (range)
T1 (1994 to 1995)	32 (12:20)	47.5 (4 to 80)	6 (18.8%) (2:4)	*P* for difference = 0.012	45.5 (4 to 73)	2 (6.3%) (1:1%)	*P* for difference = 0.003	53 (43 to 63)
T2 (1996 to 2003)	30 (6:24)	50.1 (15 to 79)	12 (40.0%) (1:11)	*P* for trend = 0.003	50.7 (20 to 73)	10 (33.3%) (0:10)	*P* for trend = 0.001	48.9 (20 to 66)
T3 (2004 to 2011)	33 (10:23)	43.6 (1 to 73)	18 (54.5%) (5:13)		40.8 (1 to 69)	14 (42.4%) (4:10)		44.4 (11 to 58)

CADM, clinically amyopathic dermatomyositis; DM, dermatomyositis; M:F, male:female; MDA-5, melanoma differentiation-associated gene 5. *Prevalence of CADM in total DM. **Prevalence of anti-MDA-5 in total DM.

the proportions of CADM and anti-MDA-5-positive patients significantly increased from the first to the third periods of the study.

Annual prevalence of CADM and anti-MDA-5 antibodies

Since many of the patients whose sera were drawn in 1994 had been treated at our hospital, the above tertile analysis was partially biased. Before the sampling in 1994 there may have been some fatal cases of rapidly progressive ILD. Moreover, some CADM patients stopped seeing their doctors due to minor illness. In light of these possibilities, we analyzed only the 72 patients who manifested the disease after 1994, in order to investigate the growing trend of CADM and anti-MDA-5-positive patients (Figure 1). The relative prevalence of both CADM and anti-MDA-5-positive patients among all DM patients was found to have significantly increased (P = 0.029 and P = 0.044, respectively).

Geographical incidence of dermatomyositis patients with anti-MDA-5 antibodies

Our university hospital is in Nagoya (population 2.2 million), the biggest city in central Japan. To clarify the regional differences in a subgroup of patients, we compared the prevalence of CADM and anti-MDA-5-positive patients by tertiles based on the population of the patient's city of residence (Table 2), and we plotted the anti-MDA-5-positive patients on a map (Figure 2). Interestingly, CADM patients were less prevalent in

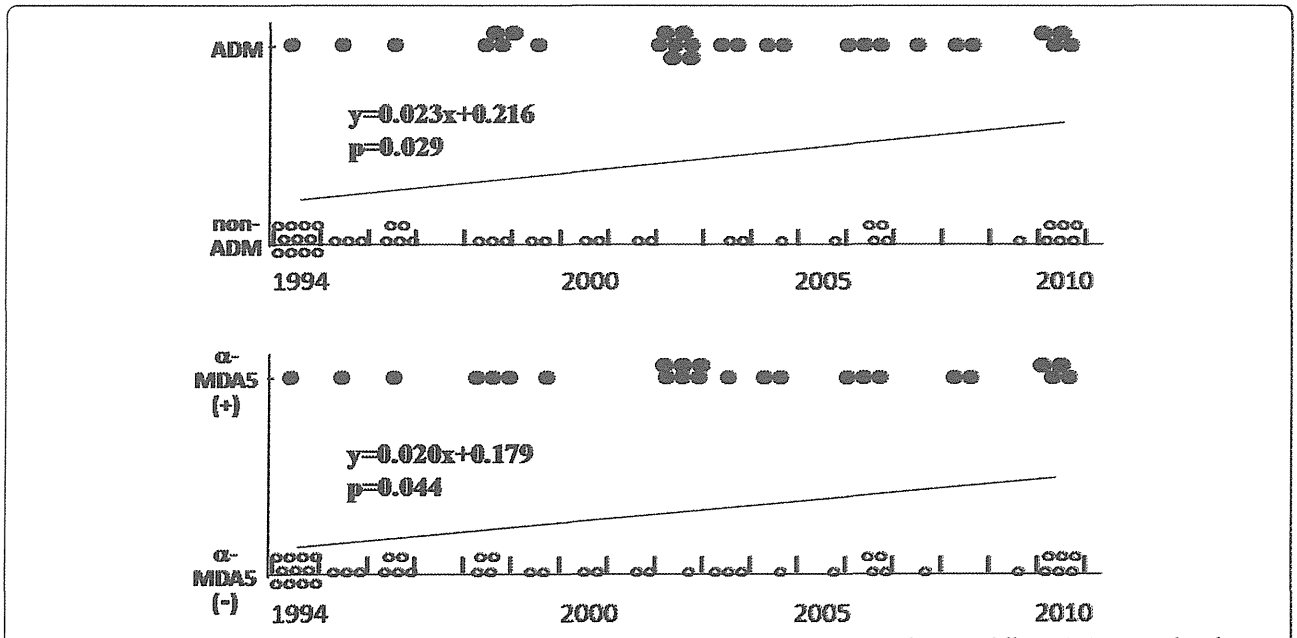

Figure 1 Annual prevalence of patients with clinically amyopathic dermatomyositis or anti-melanoma differentiation-associated gene 5 antibodies. The regression equation is shown, in which the year of disease onset is defined as 1994 = 1, 1995 = 2,..., 2010 = 17 on the *x* axis and the presence or absence of clinically amyopathic dermatomyositis (CADM) or anti-melanoma differentiation-associated gene 5 (anti-MDA-5) antibodies is defined as 1 and 0, respectively, on the *y* axis (*P* for linear trend).

Table 2 Population of the area of residence and the presence of CADM or anti-MDA-5 antibodies

			CADM			α-MDA-5-positive		
Population of area of residence (×1,000)	Total number of DM patients (M:F)	Mean age at onset (range)	Number (%) of patients (M:F)	*P* value*	Mean age at onset (range)	Number (%) of patients (M:F)	*P* value**	Mean age at onset (range)
T1 (0.5 to 108)	31 (4:27)	49.0 (4 to 70)	16 (51.6%) (1:15)	*P* for difference = 0.096	47.3 (4 to 69)	14 (45.2%) (1:13)	*P* for difference = 0.012	48.8 (20 to 66)
T2 (130 to 826)	26 (7:19)	44.0 (9 to 80)	10 (38.5%) (3:7)	*P* for trend = 0.031	40.0 (9 to 59)	7 (26.9%) (3:4)	*P* for trend = 0.003	39.9 (11 to 59)
T3 (2,200)	38 (17:21)	47.3 (1 to 79)	10 (26.3%) (4:6)		45.9 (1 to 73)	5 (13.2%) (1:4)		51.0 (39 to 63)

CADM, clinically amyopathic dermatomyositis; DM, dermatomyositis; M:F, male:female; MDA-5, melanoma differentiation-associated gene 5. *Prevalence of CADM in total DM. **Prevalence of anti-MDA-5 in total DM.

urban areas, but this association was only marginally significant, whereas there were significantly more anti-MDA-5-positive patients in rural areas than in urban ones. Areas northeast and far northwest of Nagoya contained particularly high numbers of patients with anti-MDA-5 antibodies: 10 patients in the northeast, and five patients in the northwest (Figure 2, circular dotted area). These areas had nine and six CADM patients in the northwest and northeast, respectively. All 15 patients with anti-MDA-5 antibodies were natives of the

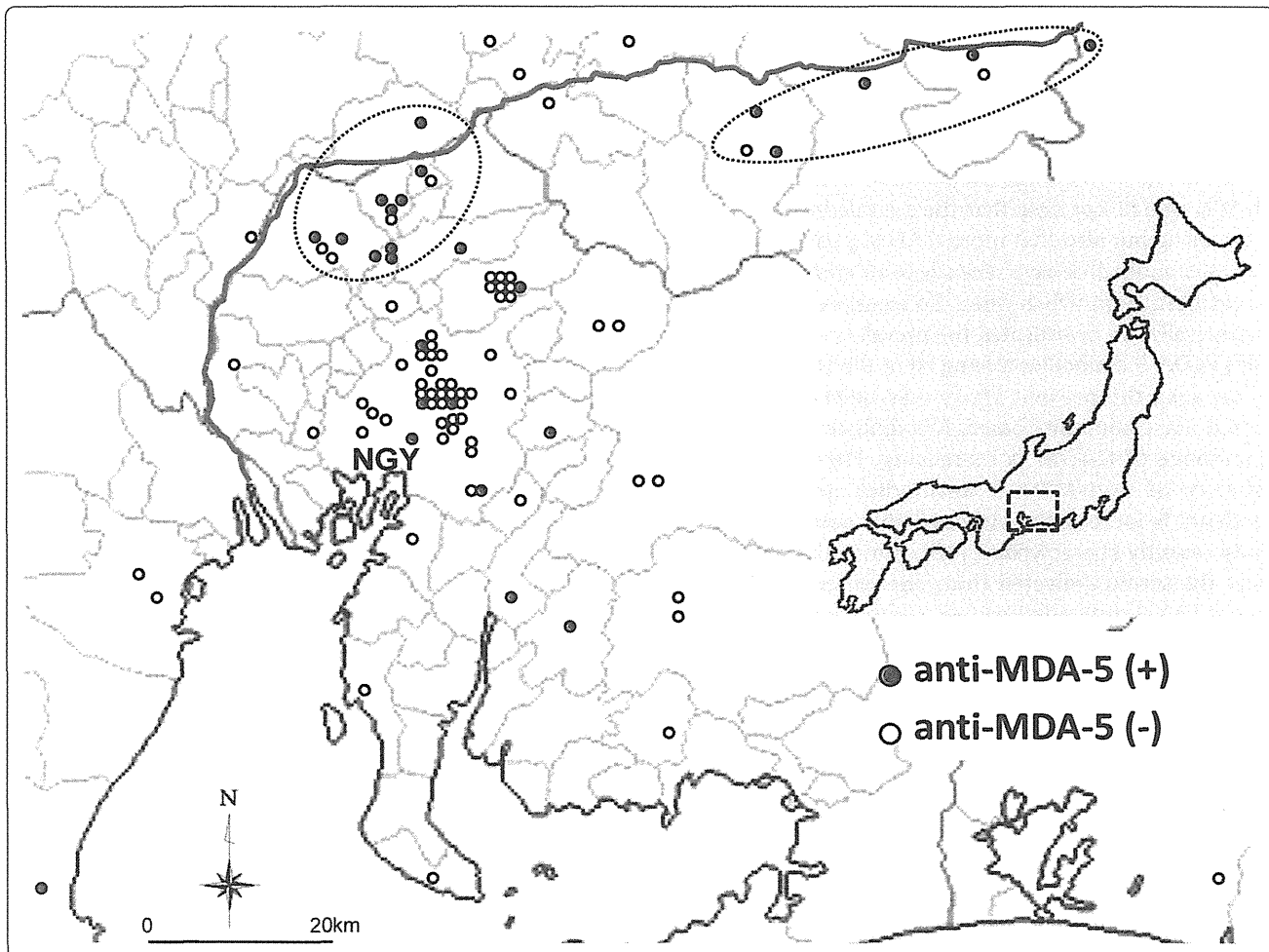

Figure 2 Geographic distribution of patients with dermatomyositis. A residential area of 95 patients was plotted. NGY, Nagoya city. Red and white circles show patients with and without anti-melanoma differentiation-associated gene 5 (anti-MDA-5) antibodies, respectively. Blue line shows the Kiso River, which is the biggest in the area.

area; five and four of these 15 patients had manifested the disease in 2002 and 2010, respectively. Notably, five of the six patients with anti-MDA-5 antibodies whose disease began in 2002 and all four of the patients with anti-MDA-5 antibodies whose disease began in 2010 were from these two areas (Figure 1).

Seasonal onset

The information on seasonality of disease onset was available for 78 patients, including 33 CADM and 25 anti-MDA-5-positive patients. There were no significant seasonal patterns of disease onset in the overall patient group or in the subgroups of male, female, CADM or anti-MDA-5-positive patients (data not shown). However, the incidence of anti-MDA-5 antibodies in areas with populations under 108×10^3, but not in areas with populations over 130×10^3, was the highest in autumn (onset in autumn in areas with populations under 108×10^3 vs. onset in autumn in areas with populations over 130×10^3 = 8/14 vs. 1/11, $P = 0.033$).

Discussion

A Japanese multicenter study confirmed recently that patients with anti-MDA-5 antibodies frequently have CADM with rapidly progressive ILD and a poor prognosis [15]. With increasing awareness of the CADM disease subtype, which was proposed by Sontheimer in the 1990s, we felt not only that the prevalence of CADM is increasing but also that more CADM patients with anti-MDA-5 antibodies have recently been coming from rural areas than from urban ones. To examine these matters statistically, we investigated the prevalence of CADM and anti-MDA-5 antibodies among all of the DM patients.

Because the present study was neither population based nor community based, it is difficult to say that the incidence of CADM is increasing. However, the frequency of anti-MDA-5 antibodies among all DM patients is increasing. Although this autoantibody was only recently characterized [8,9], our initial study found that the serum collected from one patient in 1994 was anti-MDA-5 antibody-positive. Contrary to the increasing prevalence of anti-MDA-5 antibodies, other types of autoantibodies appear to be decreasing. We also characterized the prevalence of anti-transcriptional intermediary factor-1γ antibodies among all patients examined in this study. These antibodies, however, which were detected in 12 patients, showed no significant epidemiological characteristics under the same analysis (data not shown). In our previous study using traditional immunoprecipitation experiments, we did not detect significant decreases in the prevalence of any specific autoantibodies [11]. There is little possibility that the long storage of the sera caused the autoantibodies to become less active, however, because various kinds of DM/polymyositis-specific autoantibodies were found in many of the sera that were drawn in 1994 and 1995 (two patients with anti-transcriptional intermediary factor 1γ, two patients with anti-MJ, two patients with anti-PL-7, one patient with anti-Jo-1, one patient with anti-EJ and one patient with anti-KS; our unpublished observations), along with the anti-MDA-5 antibodies found in the two other patients during this period.

MDA-5 detects some viruses, including picornaviruses, and is involved in the host defense response to infection. Antibodies to coxsackievirus B, a picornavirus, were previously reported to be prevalent in patients with juvenile DM [16]. Although we could not find an epidemiologic study on the environmental levels of picornavirus in our district, the seasonal distribution of viruses in the river water in Nara Prefecture, which is also in central Japan, has been examined [17]. The coxsackievirus B levels peaked there in the summer, and the virus continued to be detected in the autumn and winter. Interestingly, there was a marked increase in the prevalence of anti-MDA-5 antibodies in our study in areas northeast and northwest of Nagoya (Figure 2). These regions are on the Kiso River, which is the biggest river in our area (blue line in Figure 2). In these areas, there was also an accumulation of CADM. It is unlikely that sun exposure strongly contributed to the pathogenesis, because the 15 patients with CADM included only one outdoor worker.

The present study has several limitations because of the small number of study subjects. The time lag between the initial presentation of disease and the clinical assessment should be considered. The interval between disease onset and the time of sera collection in this study was not significantly different, however, between patients with and without CADM, between patients with and without anti-MDA-5 antibodies, or among the tertiles depicted in Table 1 (data not shown), suggesting that the patient follow-up periods did not differ by disease subtype. Since people in rural areas generally have reduced access to specialists, patients with severe illness, such as anti-MDA-5-positive patients, might be more prevalent in rural areas than in urban areas. Moreover, medical practices at a university hospital have an inherent referral bias.

Many reports have suggested that environmental factors play a role in the development of DM and the production of myositis-related autoantibodies (reviewed in [18]). No single factor, however, can explain that development and that production, and the possible growing prevalence of CADM and anti-MDA-5-positive patients. It seems difficult to identify environmental factors that possibly increase the annual prevalence of CADM and anti-MDA-5-positive patients, because patients could have several environmental exposures that have possible interrelationships with genetic risk factors. Various environmental

exposures require confirmation in case-controlled studies to determine which are associated with disease onset and whether these play any role in etiology.

To our knowledge, this is the first epidemiologic study on anti-MDA-5 antibodies. Although it is difficult to draw strong conclusion from a single cohort study, epidemiologic studies play an important role in disease assessment. These studies determine the extent of disease and the natural history within a community, identify potential etiologic factors and enhance our understanding of disease pathogenesis.

Conclusions

Clinically amyopathic dermatomyositis might be growing in prevalence with the increase of anti-MDA-5 antibody-positive patients in central Japan. Regional differences in the incidences of the anti-MDA-5 antibody would suggest that environmental factors contribute to the production of autoantibodies against MDA-5. It will be important to conduct larger population-based studies through multicenter collaboration using DM-specific autoantibodies to define patient groups and clarify the disease etiology associated with environmental factors.

Abbreviations

CADM: clinically amyopathic dermatomyositis; DM: dermatomyositis; ILD: interstitial lung disease; MDA-5: melanoma differentiation-associated gene 5.

Acknowledgements

The present work was supported by a grant from the Ministry of Health, Labour and Welfare of Japan and from the 24th General Assembly of the Japanese Association of Medical Sciences.

Author details

[1]Division of Connective Tissue Disease and Autoimmunity, Department of Dermatology, Nagoya University Graduate School of Medicine, 65 Tsurumai-cho, Showa-ku, Nagoya 466-8550, Japan. [2]Department of Dermatology, Nagoya Ekisaikai Hospital, 4-66 Shonen-cho, Nakagawa-ku, Nagoya 454-8502, Japan. [3]Department of Nursing, Nagoya University School of Health Sciences, 1-1-20 Daiko-Minami, Higashi-ku, Nagoya 461-8673, Japan.

Authors' contributions

YM, KS and KH organized the patient registry. YM and KH performed laboratory assays. KT participated in the design of the study and performed the statistical analysis. YM conceived of the study design and wrote the manuscript with input and consensus from all authors. KS and MA participated in the coordination of the study and helped to draft the manuscript. All authors read and approved the final manuscript.

Competing interests

The authors declare that they have no competing interests.

Received: 23 August 2011 Revised: 21 November 2011
Accepted: 22 December 2011 Published: 22 December 2011

References

1. Leff RL, Burgess SH, Miller FW, Love LA, Targoff IN, Dalakas MC, Joffe MM, Plotz PH: **Distinct seasonal patterns in the onset of adult idiopathic inflammatory myopathy in patients with anti-Jo-1 and anti-signal recognition particle autoantibodies.** *Arthritis Rheum* 1991, **34**:1391-1396.
2. Sarkar K, Weinberg CR, Oddis CV, Medsger TA Jr, Plotz PH, Reveille JD, Arnett FC, Targoff IN, Genth E, Love LA, Miller FW: **Seasonal influence on the onset of idiopathic inflammatory myopathies in serologically defined groups.** *Arthritis Rheum* 2005, **52**:2433-2438.
3. Phillips BA, Zilko PJ, Garlepp MJ, Mastaglia FL: **Seasonal occurrence of relapses in inflammatory myopathies: a preliminary study.** *J Neurol* 2002, **249**:441-444.
4. Okada S, Weatherhead E, Targoff IN, Wesley R, Miller FW, International Myositis Collaborative Study Group: **Global surface ultraviolet radiation intensity may modulate the clinical and immunologic expression of autoimmune muscle disease.** *Arthritis Rheum* 2003, **48**:2285-2293.
5. Love LA, Weinberg CR, McConnaughey DR, Oddis CV, Medsger TA Jr, Reveille JD, Arnett FC, Targoff IN, Miller FW: **Ultraviolet radiation intensity predicts the relative distribution of dermatomyositis and anti-Mi-2 autoantibodies in women.** *Arthritis Rheum* 2009, **60**:2499-2504.
6. Sontheimer RD: **Would a new name hasten the acceptance of amyopathic dermatomyositis (dermatomyositis siné myositis) as a distinctive subset within the idiopathic inflammatory dermatomyopathies spectrum of clinical illness?** *J Am Acad Dermatol* 2002, **46**:626-636.
7. Sato S, Kuwana M: **Clinically amyopathic dermatomyositis.** *Curr Opin Rheumatol* 2010, **22**:639-643.
8. Sato S, Hirakata M, Kuwana M, Suwa A, Inada S, Mimori T, Nishikawa T, Oddis CV, Ikeda Y: **Autoantibodies to a 140-kd polypeptide, CADM-140, in Japanese patients with clinically amyopathic dermatomyositis.** *Arthritis Rheum* 2005, **52**:1571-1576.
9. Sato S, Hoshino K, Satoh T, Fujita T, Kawakami Y, Fujita T, Kuwana M: **RNA helicase encoded by melanoma differentiation-associated gene 5 is a major autoantigen in patients with clinically amyopathic dermatomyositis: association with rapidly progressive interstitial lung disease.** *Arthritis Rheum* 2009, **60**:2193-2200.
10. Nakashima R, Imura Y, Kobayashi S, Yukawa N, Yoshifuji H, Nojima T, Kawabata D, Ohmura K, Usui T, Fujii T, Okawa K, Mimori T: **The RIG-I-like receptor IFIH1/MDA5 is a dermatomyositis-specific autoantigen identified by the anti-CADM-140 antibody.** *Rheumatology (Oxford)* 2010, **49**:433-440.
11. Hoshino K, Muro Y, Sugiura K, Tomita Y, Nakashima R, Mimori T: **Anti-MDA5 and anti-TIF1-γ antibodies have clinical significance for patients with dermatomyositis.** *Rheumatology (Oxford)* 2010, **49**:1726-1733.
12. Kato H, Takeuchi O, Sato S, Yoneyama M, Yamamoto M, Matsui K, Uematsu S, Jung A, Kawai T, Ishii KJ, Yamaguchi O, Otsu K, Tsujimura T, Koh CS, Reis e Sousa C, Matsuura Y, Fujita T, Akira S: **Differential roles of MDA5 and RIG-I helicases in the recognition of RNA viruses.** *Nature* 2006, **441**:101-105.
13. Bohan A, Peter JB, Bowman RL, Pearson CM: **A computer-assisted analysis of 153 patients with polymyositis and dermatomyositis.** *Medicine (Baltimore)* 1977, **56**:255-286.
14. Kobayashi I, Okura Y, Yamada M, Kawamura N, Kuwana M, Ariga T: **Anti-melanoma differentiation-associated gene 5 antibody is a diagnostic and predictive marker for interstitial lung diseases associated with juvenile dermatomyositis.** *J Pediatr* 2011, **158**:675-677.
15. Hamaguchi Y, Kuwana M, Hoshino K, Hasegawa M, Kaji K, Matsushita T, Komura K, Nakamura M, Kodera M, Suga N, Higashi A, Ogusu K, Tsutsui K, Furusaki A, Tanabe H, Sasaoka S, Muro Y, Yoshikawa M, Ishiguro N, Ayano M, Muroi E, Fujikawa K, Umeda Y, Kawase M, Mabuchi E, Asano Y, Sodemoto K, Seishima M, Yamada H, Sato S, Takehara K, Fujimoto M: **Clinical correlations with dermatomyositis-specific autoantibodies in adult Japanese patients with dermatomyositis: a multicenter cross-sectional study.** *Arch Dermatol* 2011, **147**:391-398.
16. Christensen ML, Pachman LM, Schneiderman R, Patel DC, Friedman JM: **Prevalence of Coxsackie B virus antibodies in patients with juvenile dermatomyositis.** *Arthritis Rheum* 1986, **29**:1365-1370.
17. Tani N, Dohi Y, Kurumatani N, Yonemasu K: **Seasonal distribution of adenoviruses, enteroviruses and reoviruses in urban river water.** *Microbiol Immunol* 1995, **39**:577-580.
18. Prieto S, Grau JM: **The geoepidemiology of autoimmune muscle disease.** *Autoimmun Rev* 2010, **9**:A330-A334.

doi:10.1186/ar3547
Cite this article as: Muro *et al.*: **Epidemiologic study of clinically amyopathic dermatomyositis and anti-melanoma differentiation-associated gene 5 antibodies in central Japan.** *Arthritis Research & Therapy* 2011 **13**:R214.

CELL STRUCTURE AND FUNCTION 37: 89–100 (2012)

Establishment and Characterization of Human Peripheral Nerve Microvascular Endothelial Cell Lines: A New *in vitro* Blood-Nerve Barrier (BNB) Model

Masaaki Abe[1], Yasuteru Sano[1], Toshihiko Maeda[1], Fumitaka Shimizu[1], Yoko Kashiwamura[1], Hiroyo Haruki[1], Kazuyuki Saito[2], Ayako Tasaki[1], Motoharu Kawai[1], Tetsuya Terasaki[3], and Takashi Kanda[1]*

[1]*Department of Neurology and Clinical Neuroscience, Yamaguchi University Graduate School of Medicine, 1-1-1 Minamikogushi, Ube, Yamaguchi 755-8505, Japan,* [2]*Department of Neurology and Neurological Science, Tokyo Medical and Dental University Graduate School, 1-45-45 Yushima, Bunkyo-ku, Tokyo 113-8519, Japan,* [3]*Department of Molecular Biopharmacy and Genetics, Graduate School of Pharmaceutical Sciences, Tohoku University, Aoba, Aramaki, Aoba-ku, Sendai, Miyagi 980-8578, Japan*

ABSTRACT. **The blood-nerve barrier (BNB) is a highly specialized unit that maintains the microenvironments of the peripheral nervous system. Since the breakdown of the BNB has been considered a key step in autoimmune neuropathies such as Guillain-Barré syndrome and chronic inflammatory demyelinating polyraduculoneuropathy, it is important to understand the cellular properties of the peripheral nerve microvascular endothelial cells (PnMECs) which constitute the BNB. For this purpose, we established an immortalized cell line derived from human PnMECs. The human PnMECs were transduced with retroviral vectors encoding the temperature-sensitive SV40 large T antigen and human telomerase. This cell line, termed FH-BNB, showed a spindle fiber-shaped morphology, expression of von Willebrand factor and uptake of acetylated low density lipoprotein. These cells expressed tight junction proteins including occludin, claudin-5, ZO-1 and ZO-2 at the cell-cell boundaries. P-glycoprotein and GLUT-1 were also detected by a Western blot analysis and the cells exhibited the functional expression of p-glycoprotein. In addition, transendothelial electrical resistance experiments and paracellular permeabilities of sodium fluorescein and fluorescein isothiocyanate-labeled dextran of molecular weight 4 kDa across these cells demonstrated that FH-BNBs had functional tight junctions. These results indicated that FH-BNBs had highly specialized barrier properties and they might therefore be a useful tool to analyze the pathophysiology of various neuropathies.**

Key words: blood-nerve barrier/endothelial cell lines/tight junction/transporter/claudin-5

Introduction

The blood-nerve barrier (BNB) serves as a functional and structural unit protecting the nervous system from circulating blood (Poduslo *et al.*, 1994). The BNB comprises the endoneurial microvasculature and the innermost layers of the perineurium. The perineurium is composed of flattened cells derived from fibroblasts, and these cells form several layers (Weerasuriya, 2005). Additionally, both sides of the perineurium are surrounded by basement membrane, and the perineurium is thought to be a specialized type of connective tissue (Weerasuriya, 2005). Many studies (Soderfeldt, 1974; Boddingius, 1984; Weerasuriya and Rapoport, 1986; Weerasuriya *et al.*, 1989) have demonstrated that the perineurium shows much lower permeability against many substances than endoneurial microvessels. Hence, the peripheral nerve microvascular endothelial cells (PnMECs) constituting the microvessels in the endoneurium can be considered to be the main interface between the blood and peripheral nerves. It has recently been reported that disruptions and permeability changes in the endoneurial microvessels play a crucial role in many autoimmune disorders of the peripheral nervous system including Guillain-Barré syndrome, chronic inflammatory demyelinating polyradiculoneuropathy (CIDP), and paraproteinemic neuropathy (Lach *et al.*, 1993; Kanda *et al.*,

*To whom correspondence should be addressed: Takashi Kanda, Department of Neurology and Clinical Neuroscience, Yamaguchi University Graduate School of Medicine, 1-1-1 Minamikogushi, Ube, Yamaguchi 755-8505, Japan.
Tel: +81–836–22–2714, Fax: +81–836–22–2364
E-mail: tkanda@yamaguchi-u.ac.jp

1994, 2000, 2004). Because PnMECs constitute the bulk of the BNB, *in vitro* studies using cultured PnMECs could be very useful to obtain a better understanding of the pathophysiology of these peripheral nerve disorders. However, only a few *in vitro* BNB models have been reported so far (Argall *et al.*, 1994; Kanda *et al.*, 1997; Iwasaki *et al.*, 1999; Sano *et al.*, 2007). This is probably due to the technical difficulties in isolating PnMECs from a peripheral nerve.

Transgenic rats harboring a temperature-sensitive SV40 large T-antigen gene (tsA58) have recently been developed as a source of conditionally immortalized cell lines (Takahashi *et al.*, 1999). Cultured cells derived from these animals can be easily immortalized by activating the tsA58 gene at a permissive temperature of 33°C and can have *in vivo* functions at a non-permissive temperature of 37 or 39°C (Takahashi *et al.*, 1999; Hosoya *et al.*, 2000). Human PnMECs expressing the tsA58 gene could have the potential to be used in studies elucidating their role in many diseases affecting the human peripheral nervous system. Recently, we established a conditionally immortalized PnMEC cell line derived from a human sciatic nerve and analyzed the effects of hydrocortisone on these endothelial cells (Kashiwamura *et al.*, 2011). However, the barrier properties of this cell line have not been fully characterized.

The purpose of the present study was to establish a conditionally immortalized human peripheral nerve microvascular endothelial cell line. O'Hare *et al.* reported that transgenic expression of the catalytic subunit of human telomerase (hTERT) in combination with the temperature-sensitive SV40 large T-antigen is necessary to immortalize human endothelial cells of different peripheral organs (O'Hare *et al.*, 2001). We therefore immortalized human PnMECs through coexpression of hTERT and tsA58 using retroviral vector systems, and investigated the barrier-specific properties of this novel *in vitro* BNB model.

Materials and Methods

Materials

Polyclonal anti-occludin, anti-Zonula occludens-1 (ZO-1), and anti-claudin-5 antibodies were obtained from Zymed (San Fransisco, CA, U.S.A.). The monoclonal anti-p-glycoprotein (p-gp) antibody was obtained from Signet Laboratories (Dedham, MA, U.S.A.). The polyclonal anti-Zonula occludens-2 (ZO-2) and anti-von Willebrand factor (vWF) antigen antibodies were from Santa Cruz Biotechnologies (Santa Cruz, CA, U.S.A.). The polyclonal anti-human catalytic unit of telomerase (hTERT) antigen antibodies was obtained from Rockland Immunochemicals, Inc (Gilbertsville, PA, U.S.A.). The monoclonal anti-SV40 T antigen antibody was purchased from Calbiochem (Darmstadt, Germany). Fluorescein isothiocyanate (FITC)-conjugated secondary antibodies were purchased from Zymed. The retrovirus vector pDON-AI was from TAKARA Bio Inc (Otsu, Japan). Rhodamine123, sodium fluorescein and FITC-labeled dextran of molecular weight 4 kDa were purchased from Sigma (St. Louis, MO, U.S.A.). Calcein-acetoxymethylester (calcein-AM) was obtained from Molecular Probes (Eugene, OR, U.S.A.). Verapamil was purchased from WAKO (Osaka, Japan). Human umbilical vein endothelial cells (HUVECs), HEK293 cells and HL-60 cells were obtained from Japan Health Sciences Foundation (Osaka, Japan).

Culture media

The endothelial cell (EC) growth medium contained EBM-2 medium (Cambrex, Walkersville, MD, U.S.A.) supplemented with 20% fatal bovine serum (FBS) (Highclone, Logan, UT, U.S.A.), EGM-2 MV (Cambrex), 100 U/ml penicillin (Sigma), 100 μl/ml streptomycin (Sigma), and 25 ng/ml amphotericin B (Sigma).

Isolation of human peripheral nerve microvascular endothelial cells forming the BNB

The study protocol for human peripheral nerve tissue was approved by the ethics committee of the Medical Faculty, Yamaguchi University and was conducted in compliance with the Declaration of Helsinki, as amended in Somerset West in 1996. Tissue samples were obtained from an adult female who died of a heart failure. Written informed consent was obtained from the patient's family before the study. PnMECs were isolated in accordance with a previously described procedure (Kanda *et al.*, 1997) with modification. Briefly, the sciatic nerve was removed from the patient, that the epi- and perineuria were carefully stripped off with fine forceps, mimicking the teased fiber preparation for the peripheral nerve pathology. Next, the endoneurium was finely minced with a razor blade and digested with 0.25% collagenase type I (Sigma) in 1×Hanks' balanced salt solution (HBSS) (Invitrogen) at 37°C for 2 hr in a shaking water bath. After centrifugation (800 g, 5 min), the pellet was suspended in 15% dextran solution, followed by centrifugation for 10 min at 4°C and 5,000 g. The pellet was washed and incubated in a type I collagen-coated dish (Iwaki, Chiba, Japan) at 37°C in a humidified atmosphere of 5% CO_2 and 95% air.

Immortalization and purification of PnMECs

After 4 days from the first dissemination, cells were incubated overnight with pDON-AI/tsA58, a retroviral vector encoding the open reading frame of the temperature-sensitive SV40 large T antigen. Twelve hours after the beginning of the incubation, cells were washed with HBSS and were subsequently grown at 33°C. This was followed by another overnight incubation with pDON-AI/hTERT, a retroviral vector encoding the open reading frame of hTERT. After the incubation, cells were washed with HBSS and processed for an additional incubation at 33°C. After endothelial cells (ECs) had proliferated sufficiently for cloning, they were picked up with a cloning cup. As the ECs grew, non-ECs such as pericytes, fibroblasts, and Schwann cells also appeared and gradually began to occupy the culture area of the dish. These non-ECs

were scratched and removed mechanically with a sterilized pointed rubber policeman. After several passages (passage 4) for cloning, some clonal populations that consisted of pure endothelial cells were obtained. We selected one clonal cell line which stably proliferated, and designated these cells as "FH-BNBs". These FH-BNBs showed immortality at a permissive temperature of 33°C.

Uptake of Dil-Ac-LDL

To label FH-BNBs with 1,1'-dioctacecyl-3,3,3',3', tetramethyl indocarbocyanine perchlorate acetylated low-density lipoprotein (Dil-Ac-LDL) (Biogenesis, Poole, UK), cells were incubated with 10 μg/ml Dil-Ac-LDL at 33°C in culture medium overnight. The cells were subsequently viewed under a fluorescence microscope (Olympus, Tokyo, Japan). The PnMECs had incorporated bright Dil-Ac-LDL particles into their cytoplasm. Human brain pericyte cell lines which did not take up Dil-Ac-LDL (Shimizu *et al.*, 2011) was used as a negative control.

Cell growth study

To determine the doubling time of the FH-BNBs, 5.0×10^4 cells were seeded on type I collagen-coated 35-mm dishes and grown at 33 and 37°C. After a predetermined period, the cells were trypsinized and counted using a hemocytometer.

Immunoytochemistry

The confluent cultured cells were washed twice in PBS. For von Willebrand factor immunocytochemistry, cells were fixed in 4% paraformaldehyde (Wako, Osaka, Japan) for 15 min at room temperature. Next, cells were permeabilized with 0.1% Triton X-100 (Sigma) for 10 min and then blocked with 1% FBS in PBS for 1 hr. The cells were fixed in 100% methanol for 20 min at –20°C for hTERT immunocytochemistry, were washed three times in PBS, and blocked with 1% FBS. For the staining of claudin-5, ZO-1 and ZO-2, cells were fixed with 100% ethanol for 30 min at 4°C, washed three times in PBS, permeabilized with 1% Triton X-100 for 20 min at room temperature, washed in PBS, and blocked with 2% FBS before staining. For the occludin staining, the cells were fixed with acetone and methanol mixed 1:1 for 10 min at 4°C, washed three times in PBS, and blocked with 2% FBS. After several washes with PBS, cells were incubated with the relevant antibodies (1:50 dilution) at 4°C overnight. Cells were subsequently washed with PBS and then incubated with FITC-conjugated secondary antibodies (1:200 dilutions) for 1 hr at room temperature. HUVECs were used as a negative cotrol for hTERT staining. Human brain pericyte cell lines were used as a negative control (Shimizu *et al.*, 2011). The nuclei were stained with DAPI, and fluorescence was detected using a fluorescence microscope (Olympus).

Transendothelial electrical resistance (TEER) studies

The transwell inserts (pore size, 0.4 μm; effective growth area, 30 mm^2; BD Bioscience, NJ, U.S.A.) were coated with rat tail collagen type-I (BD Bioscience) in accordance with the manufacturer's directions. Cells were seeded at 1.0×10^4 cells/insert, on these collagen-coated culture inserts and were incubated at 33°C. After attaching themselves and becoming confluent on the bottom of the insert (24–48 hr), the TEER of cell layers was measured using a Millicell electrical resistance apparatus (Endohm-6 and EVOM, World Precision Instruments, Sarasota, FL, U.S.A.). TY08 cells, which are immortalized human brain microvascular endothelial cells that have functional tight junctions (Sano *et al.*, 2010) were used as a positive control. TR-BBBs, derived from the tsA58 transgenic rat brain and lacking claudin-5 expression (Ohtsuki *et al.*, 2007) were used as control endothelial cells without sufficient barrier functions. In addition, we mesured the TEER values of FH-BNBs after 3hr incubation with 4 mM EGTA, which disrupt tight junction barrier (Li *et al.*, 2010). Statistical significance was evaluated using Student's *t*-test.

Reverse transcription-polymerase chain reaction (RT-PCR) analysis

After reaching confluency, the cells were washed three times with PBS. Total RNA was prepared from PBS-washed cells, human cerebrum and kidney using an RNeasy® Plus Mini kit (Qiagen, Hilden, Germany). RT and PCR amplification were performed with TAKARA PCR Thermal Cycler Dice (Takara, Otsu, Japan). Single-stranded cDNA was synthesized from 250 ng of total RNA using the StrataScript® First Strand Synthesis System (Stratagene, Ceda Greek, TX, U.S.A.) with an oligo-dT primer, and sequential PCR was carried out with Go Taq® (Promega). The temperature cycling conditions for each primer consisted of 5 min at 94°C, 1 min at 55–65°C, and 1 min at 72°C, with a final extension for 10 min at 72°C. The sequence specificity of each primer pair and its reference, except claudin-12, are shown in Table I. The primers for claudin-12 were designed as follows: sense ctgtttccataggcagagcg and antisense aagcagattcttagccttcc (Accession number NM_012129; fragment size 364 bp). The PCR products were visualized by ethidium bromide staining following resolution on 2% agarose gels. Products were compared with a 50-bp ladder (O'GeneRulerTM 50 bp DNA Ladder, Burlington, Canada) to estimate band size. The size of each amplified product corresponded to the expected size described in the literature.

Permeability studies

FH-BNBs, TY08 cells and TR-BBBs were seeded on 24-well tissue culture inserts (0.4 μm pore size, 1.0×10^4 cells/insert), and grown to confluence. The cells were incubated at 37°C for 30 min before the beginning of the experiment. Next, 1,300 μl of culture medium were added to the lower well and 500 μl of culture medium containing sodium fluorescein (10 μg/ml) and FITC-labeled dextran of molecular weight 4 kDa (1 mg/ml) were added to the upper compartment of each insert. After incubation for 15, 30, 45 or 60 min at 37°C, the lower chamber was sampled and the fluorescence that passed through the cell-covered inserts was mea-

Table I. HUMAN PRIMER PAIRS UTILIZED IN RT-PCR ANALYSIS

molecule	sense	antisense	reference
occludin	5'-ACCCATCTGATATGTGGAA-3'	5'-AGGAACCGGCGTGGATTTA-3'	Ghassemifar *et al.* (2003)
claudin-1	5'-CTGCCCCAGTGGAGGATTTA-3'	5'-CAATGACAGCCATCCACATC-3'	Peng *et al.* (2011)
claudin-5	5'-CTGTTTCCATAGGCAGAGCG-3'	5'-AAGCAGATTCTTAGCCTTCC-3'	Varley *et al.* (2006)
claudin-19	5'-CTCAGCGTAGTTGGCATGAA-3'	5'-GAAGAACTCCTGGGTCACCA-3'	Peng *et al.* (2011)
JAM-A	5'-GACACGGGAAGACACTGGGACA-3'	5'-ATGCGCACAGCATTTGAAGTCA-3'	Ghassemifar *et al.* (2003)
ZO-1	5'-TTTAAGCCAGCCTCTCAACA-3'	5'-CTGCTGGCTTGTTTCTCTAC-3'	Ghassemifar *et al.* (2003)
ZO-2	5'-GCCTACACTGACAATGAGCTGGA-3'	5'-TTGGGAGCATTATCTTGCTCCTCA-3'	Ghassemifar *et al.* (2003)
GLUT-1	5'-TGTCCTATCTGAGCATCGTG-3'	5'-CTCCTCGGGTCTCTTATCAC-3'	Umeki *et al.* (2002)
MDR-1	5'-GCCTGGCAGCTGGAAGACAAATACACAAAATT-3'	5'-CAGACAGCAGCTGACAGTCCAAGAACAGGACT-3'	Weksler *et al.* (2005)
MRP-1	5'-ACCAAGACGTATCAGGTGGCC-3'	5'-CTGTCTGGGCATCCAGGAT-3'	Weksler *et al.* (2005)
vWF	5'-CATTGGTGAGGATGGAGTCC-3'	5'-AGCACTGGTCTGCATTCTGG-3'	Fuchs *et al.* (2006)
G3PDH	5'-TGAAGGTCGGAGTCAACGGATTTGGT-3'	5'-CATGTGGGCCATGAGGTCCACCAC-3'	Ye *et al.* (2003)

sured using a MX3000P instrument (Stratagene). The volume cleared was plotted against time, and the slope estimated by a linear regression analysis was used to calculate the PS value for the endothelial monolayer (PeS), as described previously (Sano *et al.*, 2010): $1/PeS=1/P_{total}S-1/P_{filter}S$, where $P_{total}S$ and $P_{filter}S$ are the PS values in the presence and absence of cells, respectively. The PeS value was divided by the surface area of the culture insert (30 mm^2) to give the endothelial permeability coefficient (Pe).

Western blot (WB) analysis

FH-BNBs and human brain specimens were homogenized in cell lysis buffer containing 50 mM Tris-HCl, pH 7.4, 5 mM EDTA, 0.5% NP40, 0.5% sodium deoxycholate, 150 mM NaCl and a protease inhibitor cocktail tablet (Roche). Homogenized samples were centrifuged at 5,000 g for 10 min at 4°C and the supernatant was subjected to electrophoresis. Twenty micrograms of protein was fractionated on a 7% (p-gp), 10% (β-actin, SV40 T-antigen and GLUT-1) or 12.5% (claudin-5) gel and electophoretically transferred onto nitrocellulose membranes. The membrane was blocked at room temperature for 2 hrs with 5% powdered skimmed milk in PBS containing 0.05% Tween 20 (PBS-T). After that, the membrane was incubated with a primary antibody in PBS-T and 5% milk (1:100) at room temperature for 2 hrs, followed by incubation with a secondary antibody in PBS-T and 5% milk (1:2000) for 1 hr. Membranes were extensively washed in PBS-T and visualized by enhanced chemiluminescence detection (ECL-plus, Amersham, UK). TY08 cells that express the SV40 large T antigen and claudin-5 were used as a positive control (Sano *et al.*, 2010). HL60 cells, which do not express claudin-5, were used as a negative control, and were purchased from the Japan Health Sciences Foundation (Osaka, Japan). HEK293 cells, which do not express the SV40 large T antigen, were used as a negative control.

Drug accumulation studies

Confluent FH-BNBs grown in type I collagen-coated 24-well plates were washed three times with PBS and preincubated for 30 min at 37°C in a shaking water bath with or without verapamil (100 μM) ,which is a p-gp efflux transport inhibitor. Next, the cells were incubated in culture medium containing the fluorescent substrates rhodamine 123 (10 μM), a substrate of p-gp and Breast Cancer Resistance Protein (BCRP), or calcein-AM (10 mM), a substrate of p-gp and multi-drug resistance-associated protein 1 (MRP1) with or without verapamil for an hour at 37°C. The cells were then washed three times with PBS and lysed in 1% Triton X-100. The amount of fluorescent substrates retained in the cells was detected using a MX3000P instrument (Stratagene).

Results

Establishment of FH-BNBs

We successfully established a conditionally immortalized peripheral nerve microvascular endothelial cell line, "FH-BNB", which was obtained by transfection with a retrovirus encoding tsA58 and hTERT. FH-BNBs appeared to be closely packed and have spindle fiber-shaped morphology, which has been thought to characterize endothelial cells constituting barrier systems (Hosoya *et al.*, 2000) (Fig. 1A). Endothelial origin with FH-BNB was confirmed by their expression of von Willebrand factor and the uptake of Dil-Ac-LDL, both of which have been reported to be specific markers for endothelial cells (Yamamoto *et al.*, 1998; Voyta *et al.*, 1984). All of these cells were positive for Dil-Ac-LDL incorporation (Fig. 1A and B). The expression of factor VIII/von Willebrand factor, a specific marker for endothelial cells, on these cells was detected by RT-PCR (Fig. 1C) and immunocytochemical analysis (Fig. 1D).

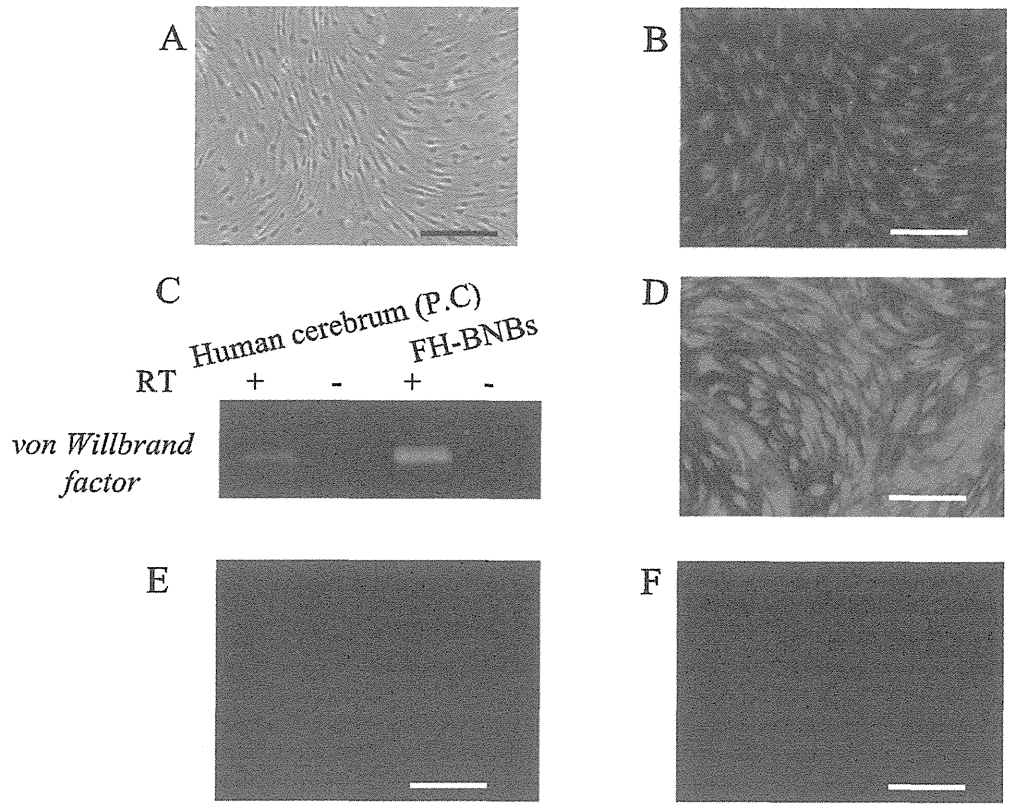

Fig. 1. A phase contrast micrograph of the FH-BNBs (A) and the corresponding fluorescence image after Dil-Ac-LDL uptake (B). The mRNA expression of von Willebrand factor (C) in FH-BNBs determinated by RT-PCR analysis. The reactions were performed against total RNA with (+) or without (–) the RT reaction. Immunostaining of FH-BNBs (D) using an anti-von Willebrand factor antibody. Human brain pericyte cells did not take up Dil-Ac-LDL (E) and express von Willebrand factor (F). The scale bars correspond to 100 μm.

Expression of tsA 58 and hTERT

In FH-BNBs, hTERT proteins were found in their nuclei (Fig. 2A and B). In addition, a WB analysis showed that these cells exhibited the large T-antigen with a molecular weight of 94 kDa, which was the same molecular weight as that of the TY08 cells used as a positive control (Fig. 2D). After the temperature shift from 33°C to 37°C, the amount of large T-antigen gradually decreased (Fig. 2D). The amount of large-T antigen protein decreased dramatically 48 hrs after the temperature shift. When FH-BNBs were seeded and cultured at 33°C, they proliferated stably with a doubling time of about 3 days (Fig. 2E) and maintained their spindle shaped morphology for more than 30 passages. However, two days after the temperature shift from 33 to 37°C, the cell growth arrested and the cells gradually swelled and finally died after a ~7-day culture (Fig. 2F). These results indicated that FH-BNBs have an obvious temperature sensitive nature and are dissimilar to cell lines expressing both the SV40 T antigen and hTERT.

Expression of tight junction molecules in FH-BNBs

The expression of claudin-1, claudin-5, claudin-12, junctional adhesion molecule A (JAM-A), ZO-1 and ZO-2 corresponding to tight junction components of endothelial cells forming BBB (Zlokovic, 2008) was verified in FH-BNBs by an RT-PCR analysis (Fig. 3A, B). Claudin-19, which deficient mice induced peripheral nervous system deficits (Miyamoto *et al.*, 2005) was expressed in FH-BNBs, but not in human cerebrum. Claudin-5, the most important barrier protein, was detected by a WB analysis at a molecular weight of 25 kDa (Fig. 3C). In addition, we showed that claudin-5, occludin, ZO-1 and ZO-2 were localized at the cell-cell boundaries in FH-BNBs by an immunohistochemical analysis (Fig. 4A–D).

Expression of transporters and functional expression of p-glycoprotein in FH-BNBs

The mRNA expression of GLUT-1, MDR1a and MRP1 were detected in FH-BNBs (Fig. 5A). In addition, GLUT-1 with a molecular weight of 55 kDa, and p-gp encoded by

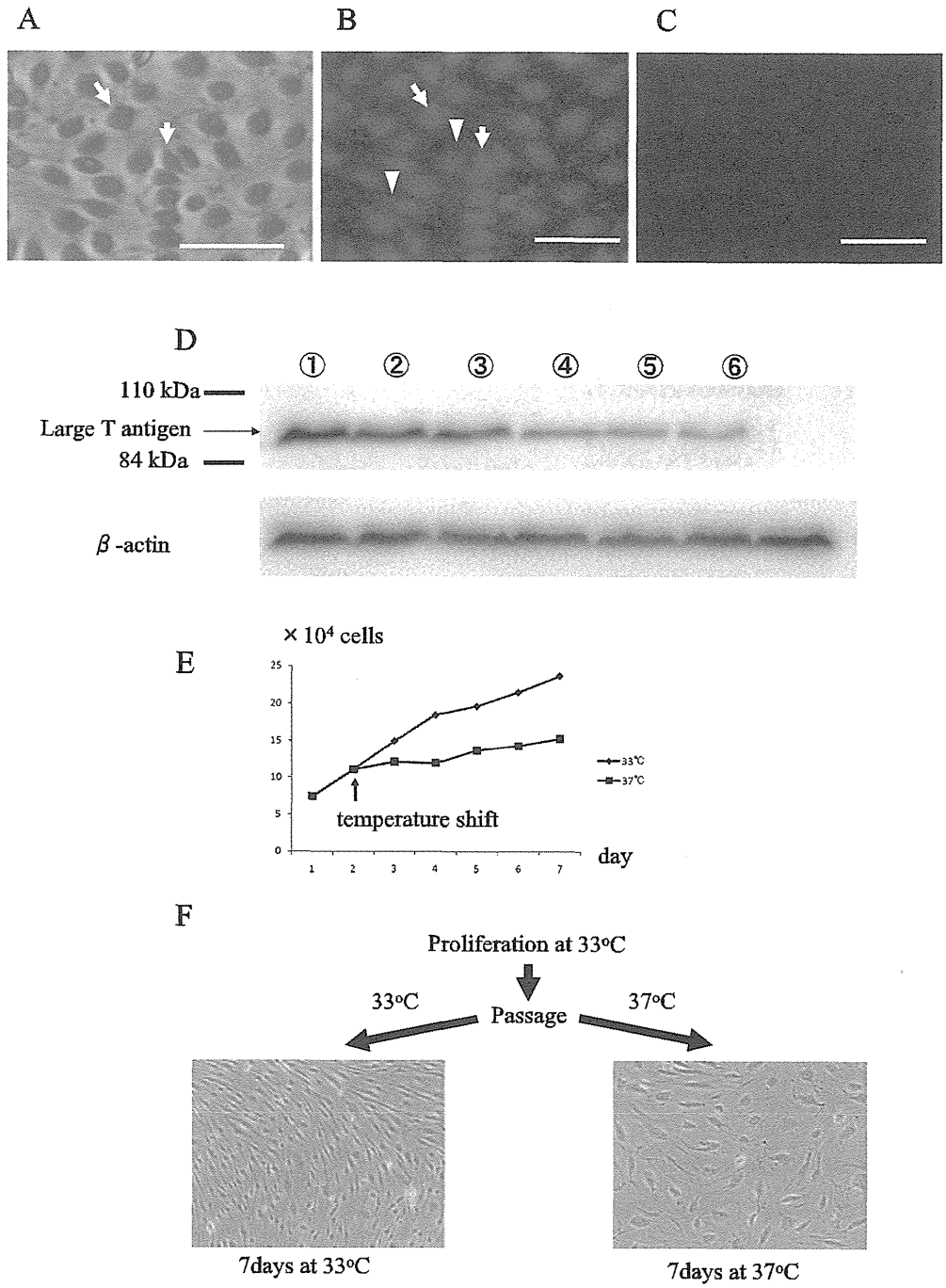

Fig. 2. A phase microscopy image of FH-BNBs (A) and the corresponding immunocytochemical staining using an anti-hTERT antibody (B). Both nuclear (arrow) and perinuclear (arrowhead) hTERT immunoreactivities were detected. HUVECs were used as a negative control for hTERT staining (C). The scale bars indicate 25 μm. The quantity of tsA58 protein (D) in FH-BNBs at permissive or non-permissive temperature was examined using an anti-SV40 large T antigen antibody. Lane 1, TY08 cells used as a positive control; Lane 2, FH-BNBs cultured at 33°C; Lane 3, FH-BNBs cultured for 24 hrs at 37°C; Lane 4, FH-BNBs cultured for 48 hrs at 37°C; Lane 5, FH-BNBs cultured for 3 days at 37°C; Lane 6, FH-BNBs cultured for 5 days at 37°C. The FH-BNBs proliferated readily at the permissive temperature of 33°C; Lane 7, HEK293 cells used as a negative control. (E). About 2 days after the temperature shift to 37°C, the cell growth was arrested. Each point represents the mean±standard deviation (SD, n=3). The temperature sensitive nature of FH-BNBs (F). This cell line demonstrated sufficient proliferation at the permissive temperature (33°C). However, once the cells are spread at the dish at 37°C, they gradually lose their proliferative capacity and become senescent and enlarged. This morphology resembles non-transfected, primary cultured human PnMECs.

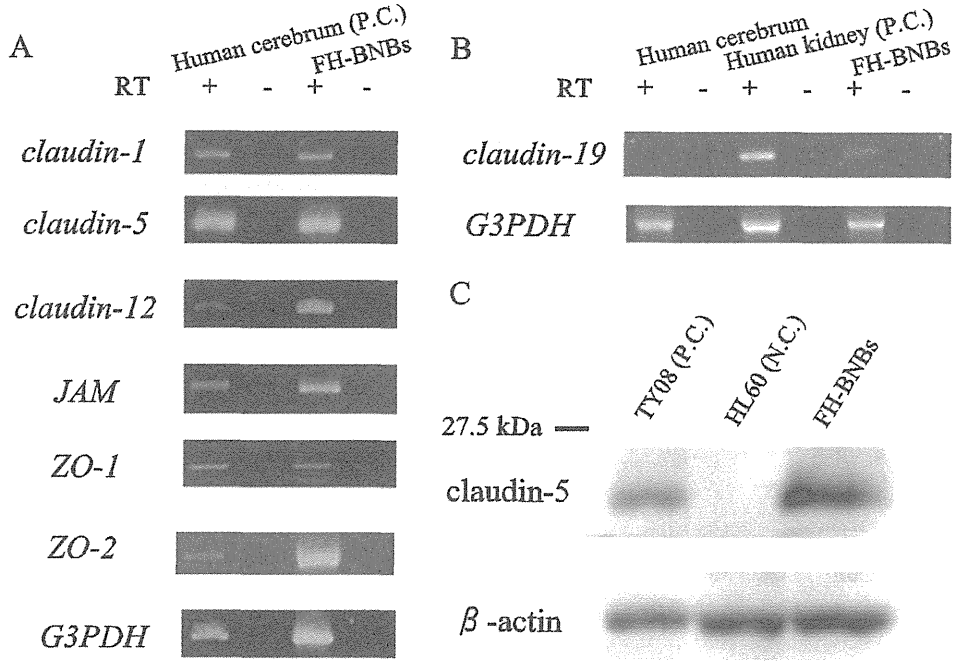

Fig. 3. The RT-PCR analysis of the expression of tight junction molecules in FH-BNBs. The expression of claudin-1, claudin-5, claudin-12, JAM-A, ZO-1 and ZO-2 mRNA in human brain specimens (lane 1) and FH-BNBs (lane 2) were verified (A). Claudin-19 mRNA were expressed in human kidney specimens (lane 2) and FH-BNBs (lane 3) but not human cerebrum specimens (lane 1) (B). G3PDH was used as a control. The reactions were performed against total RNA with (+) or without (–) RT. The Western blot analysis of claudin-5 in FH-BNBs (C). Lane 1, TY08 cells used as a positive control; Lane 2, HL-60 cells as a negative control; Lane 3, FH-BNBs.

MDR-1 with a molecular weight of 190 kDa, were verified in FH-BNBs at the protein level by a WB analysis (Fig. 5B). Next, the function of p-gp was evaluated in the FH-BNBs. The influence of the p-gp inhibitor verapamil on the uptake of the p-gp substrates rhodamine 123 and calcein-AM in the FH-BNBs was investigated. The inhibition of p-gp by verapamil led to a significantly increased uptake of rhodamine123 (Fig. 6A) and calcein-AM (Fig. 6B). These results therefore showed that the p-gp expressed in the FH-BNBs acted as an efflux pump against the p-gp substrates.

FH-BNBs have functional tight junctions

Compared with TY08 cells, which express claudin-5 and have functional tight junctions (Sano *et al.*, 2010), FH-BNBs demonstrated the similar degrees of the permeability coefficients for sodium fluorescein (MW=376 Da; 0.60±0.16 vs 0.34±0.03×10^{-3} cm/min) (Fig. 7A) and FITC-dextran (MW=4 kDa; 0.34±0.12 vs 0.30±0.09×10^{-3} cm/min) (Fig. 7B), as well as similar TEER values (36.3±4.0 vs 38.0±4.4 Ω.cm^2) (Fig. 7C). In addition, the permeabilities to each of the above compounds were much lower than those of TR-BBBs and the TEER value of FH-BNBs was much higher than that of the TR-BBBs, which have been reported to lose their barrier properties due to a lack of claudin-5 expression (Ohtsuki *et al.*, 2007). The TEER values of FH-BNBs incubated with 4 mM EGTA, which disrupt tight junction barrier (Li *et al.*, 2010), decreased and became comparable to those of TR-BBBs (Fig. 7C). These results indicate that FH-BNBs have the same degree of functional tight junctions as TY08 cells.

Discussion

In this study, we successfully established a human peripheral nerve microvascular endothelial cell line (FH-BNBs). Since primary PnMECs rapidly undergo senescence after a few divisions (Kanda *et al.*, 1997), it is very difficult to establish stable experimental systems using primary cell culture. Usually, oncogenes such as the SV40 large T-antigen, have been used to immortalize human somatic cells like brain microvascular endothelial cells (Stins *et al.*, 2001). However, the SV40 large T-antigen interacts with various proteins such as retinoblastoma and p53, and these interactions often affect fundamental cellular functions. In fact, one of the endothelial cell lines immortalized by the SV40 large T-antigen did not show contact inhibition, i.e. they demonstrated a tumor-like phenotype (Callahan *et al.*, 2004). To overcome these problems, we have immortalized

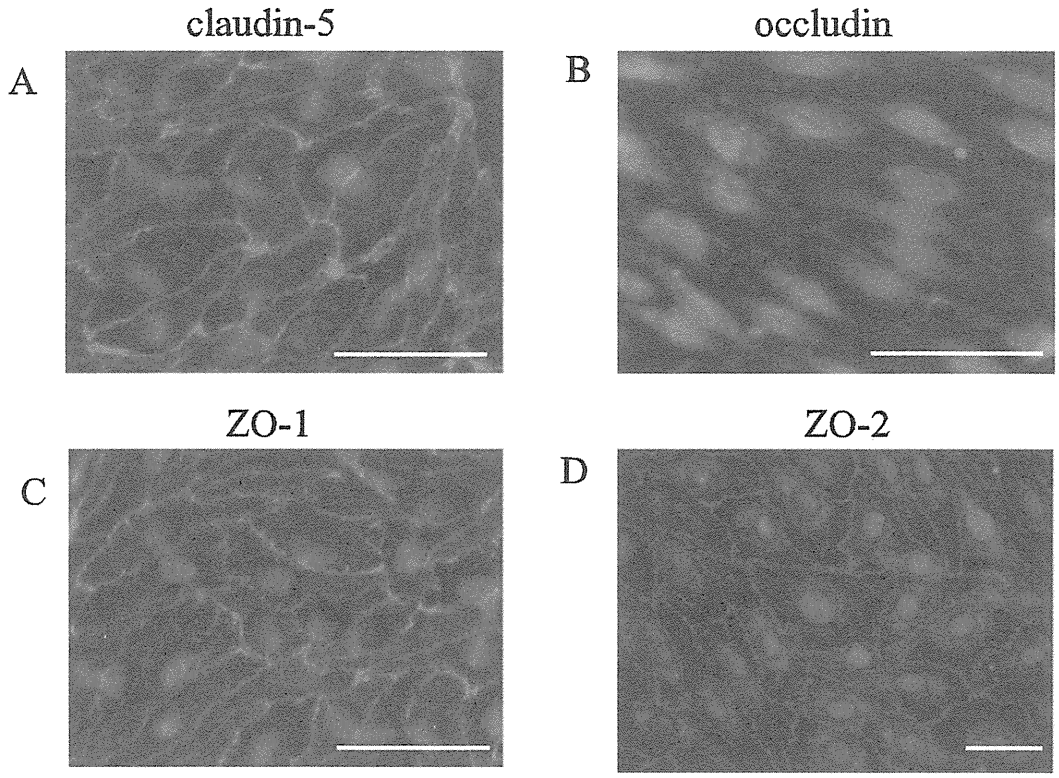

Fig. 4. Immunocytochemical analysis of tight junction proteins in confluent FH-BNBs. Claudin-5 (A), occludin (B), ZO-1 (C) and ZO-2 (D) were continuously detected at the cell-cell boundaries in FH-BNBs. Their nuclei were stained with DAPI (blue). The scale bars indicate 25 μm.

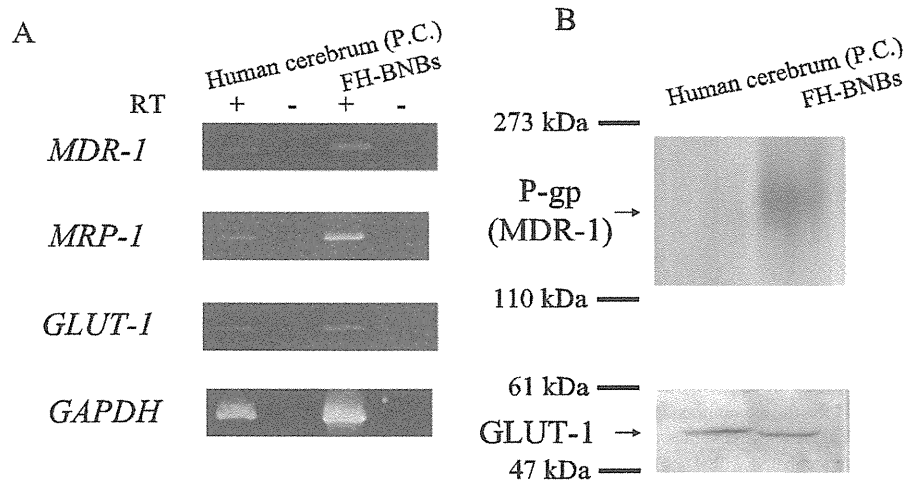

Fig. 5. (A) The expression of transporters in FH-BNBs. G3PDH was used as a control. MDR-1, MRP-1 and GLUT-1 mRNA were all detected in human brain samples as well as in FH-BNBs. The reaction were performed against total RNA with (+) or without (–) RT. (B) The Western blot analysis of the expression of p-gp and GLUT-1 in FH-BNBs. Lane 1, human cerebral cortex as a positive control; Lane 2, FH-BNBs.

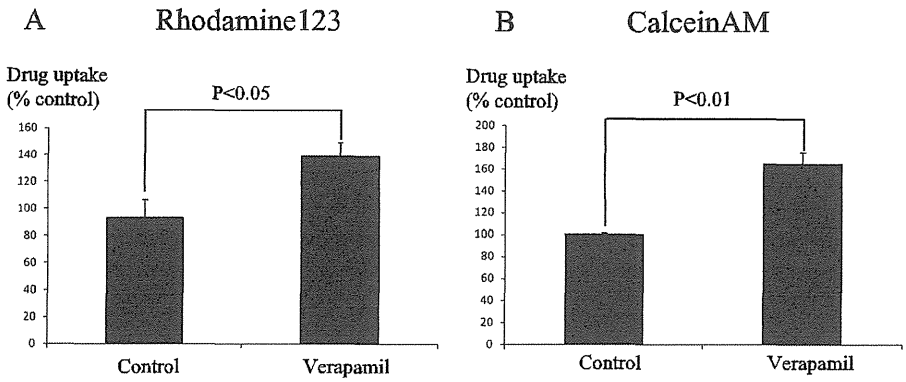

Fig. 6. The result of the p-gp functional assay in FH-BNBs. The cellular uptake of rhodamine123 (A) and calceinAM (B), which are substrates of p-gp was measured in the presence or absence of verapamil, a specific inhibitor of p-gp. The uptake of rhodamine123 and calceinAM in the presence of verapamil was significantly higher than that of control cells without verapamil. The experiments were performed in triplicate. The data are presented as the means and SD.

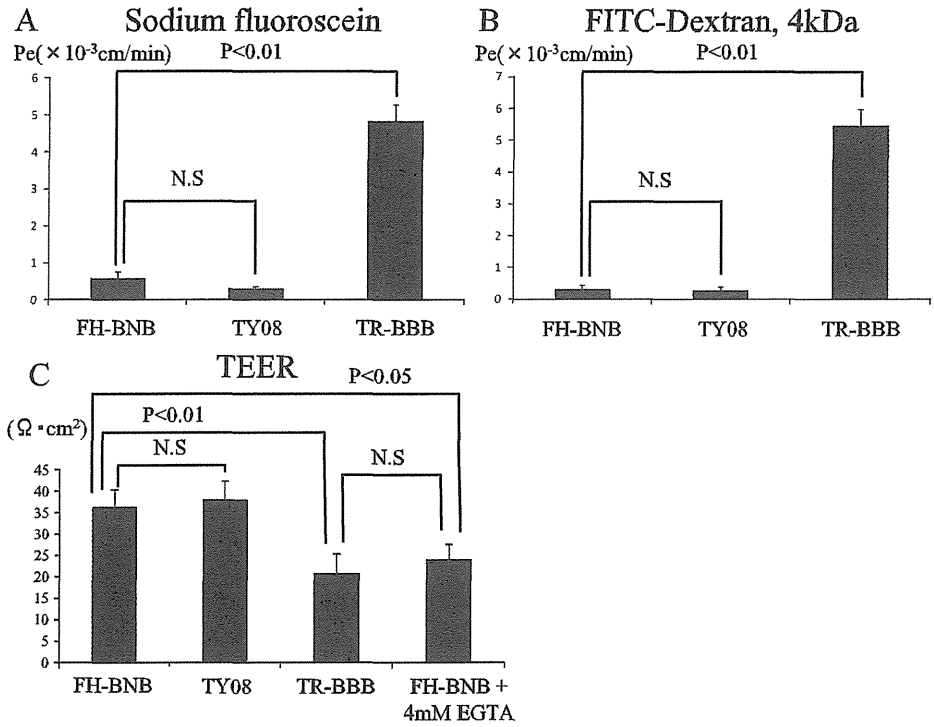

Fig. 7. The paracellular transport of sodium fluorescein (A) and FITC-dextran (B) in FH-BNBs, TY08 cells and the TR-BBBs. The permeability coefficients (Pe) of FH-BNBs for these compounds were as low as those of TY08 cells, and were much lower than those of the TR-BBBs. (C) The transendothelial electrical resistance (TEER) values of the FH-BNBs were as high as those of the TY08 cells, and were higher than those of the TR-BBBs. The TEER values of FH-BNBs incubated with 4 mM EGTA decreaced and became comparable to those of TR-BBBs. The experiments were performed in triplicate. The data are presented as the means±SD.

primary human PnMECs a using temperature-sensitive SV 40 large T antigen (tsA58) and the catalytic subunit of human telomerase (hTERT). FH-BNBs, which express both the hTERT protein and the tsA58 protein, showed a temperature-sensitive nature (Fig. 2E). They grow stably under the permissive temperature of 33°C and stop growing under the non-permissive temperature of 37°C. FH-BNBs showed spindle fiber morphology and contact inhibition even under the permissive temperature of 33°C, indicating that FH-BNBs, even at the permissive temperature, did not

develop a tumor-like phenotype.

The endothelial cells forming the BBB express many TJ-associated molecules including occludin (Furuse *et al.*, 1993), claudin-1 (Pfeiffer *et al.*, 2011), claudin-5 (Nitta *et al.*, 2003), claudin-12 (Nitta *et al.*, 2003; Ohtsuki *et al.*, 2007), ZO-1, ZO-2 (Biernacki *et al.*, 2004) and JAM-A (Yeung *et al.*, 2008). These molecules compose TJs and limit the paracellular permeability in order to maintain the brain microenvironment. Previous reports have indicated that PnMECs in human sural nerves express occludin, claudin-5 and ZO-1 (Kanda *et al.*, 2004), and claudin-1 was detected in perineurium (Hirakawa *et al.*, 2003), primary human PnMECs (Yosef *et al.*, 2010) and human Schwann cells (Alanne *et al.*, 2009). We also reported that rat PnMECs expressed many molecules forming tight junctions (Sano *et al.*, 2007). FH-BNBs expressed all of the important molecules for maintaining tight junctions at the mRNA level, and contained occludin, claudin-5, ZO-1 and ZO-2 at the cell-cell boundaries at the protein level. Claudin-19 was expressed in human retinal pigment epithelium (Peng *et al.*, 2011) and mouse sciatic nerve and kidney, but not in brain (Miyamoto *et al.*, 2005). Furthermore, claudin-19 existed in peripheral myelinated axons and claudin-19 deficient mice induced peripheral nervous system deficits (Miyamoto *et al.*, 2005). We firstly demonstrated that human PnMECs express claudin-19, indicating that claudin-19 might be a factor to differentiate the endothelial cells of BNB from those of BBB. Trans endothelial permeability studies in FH-BNBs demonstrated that these cells have a barrier function similar to TY08 cells. Furthermore, the TEER values and permeability to FITC-labeled dextran (MW=4 kDa) were similar to those of hCMEC/D3 cells (TEER 36.3±4.0 vs 30–40 $\Omega.cm^2$; Pe 0.34±0.12 vs 0.325×10^{-3} cm/min), which are human brain microvascular endothelial cell lines that maintain functional tight junctions (Weksler *et al.*, 2005). In the case of sodium fluorescein, the permeability of the FH-BNBs was lower than that of the hCMEC/D3 cells ($0.60\pm0.16\times10^{-3}$ cm/min vs 2.36×10^{-4} cm/sec) (Hsuchou *et al.*, 2010). Consequently, the FH-BNBs were thought to form an effective barrier similar to the BBB forming endothelial cell lines, TY08 and hCMEC/D3 cells. It has been reported that immortalized endothelial cell lines derived from mouse, bovine, rat, porcine BBB show high TEER values (Deli *et al.*, 2005). On the other hand, the TEER of hCMEC/D3 cells and TY08 cells, both of which were derived from human brain, have been reported to be 30–40 ohm cm^2 (Weksler *et al.*, 2005; Sano *et al.*, 2010). We think that this discrepancy of the TEER values might result from a species differences. Another considerable point is the problem of purity of the cells. Yosef *et al.* reported that primary human PnMECs have higher TEER values than FH-BNBs (Yosef *et al.*, 2010). However, these primary cells inevitably contained a small amount of pericytes, which have been reported to promote barrier integrity of the barrier-derived endothelial cells (Shimizu *et al.*, 2011). Because the purity of FH-BNBs, TY08, and hCMEC/D3 is 100% and all of these cell lines are derived from humans, we think that FH-BNBs have functional tight junctions as barrier-constituting cells derived from human tissue.

In the brain, ABC transporters such as p-gp and MRP-1 are mainly localized on the luminal surface of endothelial cells, and quickly remove the toxic metabolites to maintain brain homeostasis (Schinkel *et al.*, 1996). GLUT-1, a D-glucose transporter, is abundantly present on the abluminal surface of endothelial cells forming the BBB. GLUT-1 plays important roles in brain metabolism, since glucose is the main energy source in the brain (Qutub and Hunt, 2005; Simpson *et al.*, 2007). The glucose requirements of peripheral nerves have been also reported to be very high (Greene and Winegrad, 1979). We previously described that the same transporters were expressed in rat PnMECs (Sano *et al.*, 2007). GLUT-1 and p-gp have been demonstrated to present on microvessels in the endoneurium of rat sciatic nerves by an immunohistochemical analysis (Sano *et al.*, 2007). The FH-BNBs in the present study also expressed MDR-1, MRP-1 and GLUT-1. In addition, the functional expression of p-gp was observed in these cells. These results suggest that PnMECs supply D-glucose as an energy source for nerve fibers by using GLUT-1, and protect nerve tissues against toxic substrates with p-gp in the peripheral nervous system.

Recently, primary cultured human PnMECs were isolated and extensively characterized (Yosef *et al.*, 2010). These cells are very useful to analyze the nature of the endothelium forming the BNB; however, they have limited capacities for division because they are not immortalized, and they also contain a small percentage of non-endothelial cells including pericytes and fibroblasts. On the other hand, our FH-BNBs consist of 100% endothelial cells derived from the BNB and have the ability to grow and maintain their barrier phenotype after at least 30 passages.

In conclusion, the newly established FH-BNBs, which maintain their original nature as endothelial cells forming the BNB will be a useful tool for investigating the biology of the human BNB, and may lead to the development of novel therapies for many autoimmune and other neuropathies.

Acknowledgments. This study was supported in part by research grants (No.21390268, 21790841 and 22790821) from the Japan Society for the Promotion of Science, Tokyo, Japan.

References

Alanne, M.H., Pummi, K., Heape, A.M., Grenman, R., Peltonen, J., and Peltonen, S. 2009. Tight junction proteins in human Schwann cell autotypic junctions. *J. Histochem. Cytochem.*, **57**: 523–529.

Argall, K.G., Armati, P.J., and Pollard, J.D. 1994. A method for the isolation and culture of rat peripheral nerve vascular endothelial cells. *Mol. Cell. Neurosci.*, **5**: 413–417.

Biernacki, K., Prat, A., Blain, M., and Antel, J.P. 2004. Regulation of cellular and molecular trafficking across human brain endothelial cells

by Th1- and Th2-polarized lymphocytes. *J. Neuropathol. Exp. Neurol.*, **63**: 223–232.

Boddingius, J. 1984. Ultrastructural and histophysiological studies on the blood-nerve barrier and perineurial barrier in leprosy neuropathy. *Acta Neuropathol.*, **64**: 282–296.

Callahan, M.K., Williams, K.A., Kivisakk, P., Pearce, D., Stins, M.F., and Ransohoff, R.M. 2004. CXCR3 marks CD4+ memory T lymphocytes that are competent to migrate across a human brain microvascular endothelial cell layer. *J. Neuroimmunol.*, **153**: 150–157.

Deli, M.A., Abraham, C.S., Kataoka, Y., and Niwa, M. 2005. Permeability studies on in vitro blood-brain barrier models: physiology, pathology, and pharmacology. *Cell Mol. Neurobiol.*, **25**: 59–127.

Fuchs, S., Hermanns, M.I., and Kirkpatrick, C.J. 2006. Retention of a differentiated endothelial phenotype by outgrowth endothelial cells isolated from human peripheral blood and expanded in long-term cultures. *Cell Tissue Res.*, **326**: 79–92.

Furuse, M., Hirase, T., Itoh, M., Nagafuchi, A., Yonemura, S., Tsukita, S., and Tsukita, S. 1993. Occludin: a novel integral membrane protein localizing at tight junctions. *J. Cell Biol.*, **123**: 1777–1788.

Ghassemifar, M.R., Eckert, J.J., Houghton, F.D., Picton, H.M., Leese, H.J., and Fleming, T.P. 2003. Gene expression regulating epithelial intercellular junction biogenesis during human blastocyst development in vitro. *Mol. Hum. Reprod.*, **9**: 245–252.

Greene, D.A. and Winegrad, A.I. 1979. In vitro studies of the substrates for energy production and the effects of insulin on glucose utilization in the neural components of peripheral nerve. *Diabetes*, **28**: 878–887.

Hirakawa, H., Okajima, S., Nagaoka, T., Takamatsu, T., and Oyamada, M. 2003. Loss and recovery of the blood-nerve barrier in the rat sciatic nerve after crush injury are associated with expression of intercellular junctional proteins. *Exp. Cell Res.*, **284**: 196–210.

Hosoya, K.I., Takashima, T., Tetsuka, K., Nagura, T., Ohtsuki, S., Takanaga, H., Ueda, M., Yanai, N., Obinata, M., and Terasaki, T. 2000. mRna expression and transport characterization of conditionally immortalized rat brain capillary endothelial cell lines; a new in vitro BBB model for drug targeting. *J. Drug Target.*, **8**: 357–370.

Hsuchou, H., Kastin, A.J., Tu, H., Joan Abbott, N., Couraud, P.O., and Pan, W. 2010. Role of astrocytic leptin receptor subtypes on leptin permeation across hCMEC/D3 human brain endothelial cells. *J. Neurochem.*, **115**: 1288–1298.

Iwasaki, T., Kanda, T., and Mizusawa, H. 1999. Effects of pericytes and various cytokines on integrity of endothelial monolayer originated from blood-nerve barrier: an in vitro study. *J. Med. Dent. Sci.*, **46**: 31–40.

Kanda, T., Yoshino, H., Ariga, T., Yamawaki, M., and Yu, R.K. 1994. Glycosphingolipid antigens in cultured bovine brain microvascular endothelial cells: sulfoglucuronosyl paragloboside as a target of monoclonal IgM in demyelinative neuropathy. *J. Cell Biol.*, **126**: 235–246.

Kanda, T., Iwasaki, T., Yamawaki, M., and Ikeda, K. 1997. Isolation and culture of bovine endothelial cells of endoneurial origin. *J. Neurosci. Res.*, **49**: 769–777.

Kanda, T., Yamawaki, M., Iwasaki, T., and Mizusawa, H. 2000. Glycosphingolipid antibodies and blood-nerve barrier in autoimmune demyelinative neuropathy. *Neurology*, **54**: 1459–1464.

Kanda, T., Numata, Y., and Mizusawa, H. 2004. Chronic inflammatory demyelinating polyneuropathy: decreased claudin-5 and relocated ZO-1. *J. Neurol. Neurosurg. Psychiatry*, **75**: 765–769.

Kashiwamura, Y., Sano, Y., Abe, M., Shimizu, F., Haruki, H., Maeda, T., Kawai, M., and Kanda, T. 2011. Hydrocortisone enhances the function of the blood-nerve barrier through the up-regulation of claudin-5. *Neurochem. Res.*, **36**: 849–855.

Lach, B., Rippstein, P., Atack, D., Afar, D.E., and Gregor, A. 1993. Immunoelectron microscopic localization of monoclonal IgM antibodies in gammopathy associated with peripheral demyelinative neuropathy. *Acta Neuropathol.*, **85**: 298–307.

Li, M.W., Mruk, D.D., Lee, W.M., and Cheng, C.Y. 2010. Connexin 43 is critical to maintain the homeostasis of the blood-testis barrier via its effects on tight junction reassembly. *Proc. Natl. Acad. Sci. USA*, **107**: 17998–18003.

Miyamoto, T., Morita, K., Takemoto, D., Takeuchi, K., Kitano, Y., Miyakawa, T., Nakayama, K., Okamura, Y., Sasaki, H., Miyachi, Y., Furuse, M., and Tsukita, S. 2005. Tight junctions in Schwann cells of peripheral myelinated axons: a lesson from claudin-19-deficient mice. *J. Cell Biol.*, **169**: 527–538.

Nitta, T., Hata, M., Gotoh, S., Seo, Y., Sasaki, H., Hashimoto, N., Furuse, M., and Tsukita, S. 2003. Size-selective loosening of the blood-brain barrier in claudin-5-deficient mice. *J. Cell Biol.*, **161**: 653–660.

O'Hare, M.J., Bond, J., Clarke, C., Takeuchi, Y., Atherton, A.J., Berry, C., Moody, J., Silver, A.R., Davies, D.C., Alsop, A.E., Neville, A.M., and Jat, P.S. 2001. Conditional immortalization of freshly isolated human mammary fibroblasts and endothelial cells. *Proc. Natl. Acad. Sci. USA*, **98**: 646–651.

Ohtsuki, S., Sato, S., Yamaguchi, H., Kamoi, M., Asashima, T., and Terasaki, T. 2007. Exogenous expression of claudin-5 induces barrier properties in cultured rat brain capillary endothelial cells. *J. Cell Physiol.*, **210**: 81–86.

Peng, S., Rao, V.S., Adelman, R.A., and Rizzolo, L.J. 2011. Claudin-19 and the barrier properties of the human retinal pigment epithelium. *Invest. Ophthalmol. Vis. Sci.*, **52**: 1392–1403.

Pfeiffer, F., Schafer, J., Lyck, R., Makrides, V., Brunner, S., Schaeren-Wiemers, N., Deutsch, U., and Engelhardt, B. 2011. Claudin-1 induced sealing of blood-brain barrier tight junctions ameliorates chronic experimental autoimmune encephalomyelitis. *Acta Neuropathol.*, **122**: 601–614.

Poduslo, J.F., Curran, G.L., and Berg, C.T. 1994. Macromolecular permeability across the blood-nerve and blood-brain barriers. *Proc. Natl. Acad. Sci. USA*, **91**: 5705–5709.

Qutub, A.A. and Hunt, C.A. 2005. Glucose transport to the brain: a systems model. *Brain Res. Brain Res. Rev.*, **49**: 595–617.

Sano, Y., Shimizu, F., Nakayama, H., Abe, M., Maeda, T., Ohtsuki, S., Terasaki, T., Obinata, M., Ueda, M., Takahashi, R., and Kanda, T. 2007. Endothelial cells constituting blood-nerve barrier have highly specialized characteristics as barrier-forming cells. *Cell Struct. Funct.*, **32**: 139–147.

Sano, Y., Shimizu, F., Abe, M., Maeda, T., Kashiwamura, Y., Ohtsuki, S., Terasaki, T., Obinata, M., Kajiwara, K., Fujii, M., Suzuki, M., and Kanda, T. 2010. Establishment of a new conditionally immortalized human brain microvascular endothelial cell line retaining an in vivo blood-brain barrier function. *J. Cell. Physiol.*, **225**: 519–528.

Schinkel, A.H., Wagenaar, E., Mol, C.A., and van Deemter, L. 1996. P-glycoprotein in the blood-brain barrier of mice influences the brain penetration and pharmacological activity of many drugs. *J. Clin. Invest.*, **97**: 2517–2524.

Shimizu, F., Sano, Y., Abe, M.A., Maeda, T., Ohtsuki, S., Terasaki, T., and Kanda, T. 2011. Peripheral nerve pericytes modify the blood-nerve barrier function and tight junctional molecules through the secretion of various soluble factors. *J. Cell. Physiol.*, **226**: 255–266.

Simpson, I.A., Carruthers, A., and Vannucci, S.J. 2007. Supply and demand in cerebral energy metabolism: the role of nutrient transporters. *J. Cereb. Blood Flow Metab.*, **27**: 1766–1791.

Soderfeldt, B. 1974. The perineurium as a diffusion barrier to protein tracers. Influence of histamine, serotonine and bradykinine. *Acta Neuropathol.*, **27**: 55–60.

Stins, M.F., Badger, J., and Sik Kim, K. 2001. Bacterial invasion and transcytosis in transfected human brain microvascular endothelial cells. *Microb. Pathog.*, **30**: 19–28.

Takahashi, R., Hirabayashi, M., Yanai, N., Obinata, M., and Ueda, M. 1999. Establishment of SV40-tsA58 transgenic rats as a source of conditionally immortalized cell lines. *Exp. Anim.*, **48**: 255–261.

Umeki, N., Fukasawa, Y., Ohtsuki, S., Hori, S., Watanabe, Y., Kohno, Y., and Terasaki, T. 2002. mRNA expression and amino acid transport characteristics of cultured human brain microvascular endothelial cells (hBME). *Drug Metab. Pharmacokinet.*, **17**: 367–373.

Varley, C.L., Garthwaite, M.A., Cross, W., Hinley, J., Trejdosiewicz, L.K., and Southgate, J. 2006. PPARgamma-regulated tight junction development during human urothelial cytodifferentiation. *J. Cell. Physiol.*, **208**: 407–417.

Voyta, J.C., Via, D.P., Butterfield, C.E., and Zetter, B.R. 1984. Identification and isolation of endothelial cells based on their increased uptake of acetylated-low density lipoprotein. *J. Cell Biol.*, **99**: 2034–2040.

Weerasuriya, A. and Rapoport, S.I. 1986. Endoneurial capillary permeability to [14C]sucrose in frog sciatic nerve. *Brain Res.*, **375**: 150–156.

Weerasuriya, A., Curran, G.L., and Poduslo, J.F. 1989. Blood-nerve transfer of albumin and its implications for the endoneurial microenvironment. *Brain Res.*, **494**: 114–121.

Weerasuriya, A. 2005. Blood-Nerve Interface and Endoneurial Homeostasis. Peripheral neuropathy (P.J. Dick and P.K. Thomas, eds.). Elsevier, Philadelphia, pp.651–665.

Weksler, B.B., Subileau, E.A., Perriere, N., Charneau, P., Holloway, K., Leveque, M., Tricoire-Leignel, H., Nicotra, A., Bourdoulous, S., Turowski, P., Male, D.K., Roux, F., Greenwood, J., Romero, I.A., and Couraud, P.O. 2005. Blood-brain barrier-specific properties of a human adult brain endothelial cell line. *FASEB J.*, **19**: 1872–1874.

Yamamoto, K., de Waard, V., Fearns, C., and Loskutoff, D.J. 1998. Tissue distribution and regulation of murine von Willebrand factor gene expression in vivo. *Blood*, **92**: 2791–2801.

Ye, L., Martin, T.A., Parr, C., Harrison, G.M., Mansel, R.E., and Jiang, W.G. 2003. Biphasic effects of 17-beta-estradiol on expression of occludin and transendothelial resistance and paracellular permeability in human vascular endothelial cells. *J. Cell. Physiol.*, **196**: 362–369.

Yeung, D., Manias, J.L., Stewart, D.J., and Nag, S. 2008. Decreased junctional adhesion molecule-A expression during blood-brain barrier breakdown. *Acta Neuropathol.*, **115**: 635–642.

Yosef, N., Xia, R.H., and Ubogu, E.E. 2010. Development and characterization of a novel human in vitro blood-nerve barrier model using primary endoneurial endothelial cells. *J. Neuropathol. Exp. Neurol.*, **69**: 82–97.

Zlokovic, B.V. 2008. The blood-brain barrier in health and chronic neurodegenerative disorders. *Neuron*, **57**: 178–201.

(Received for publication, December 5, 2011, accepted, May 8, 2012 and published online, May 19, 2012)

doi:10.1093/brain/aws106 Brain 2012: 135; 1767–1777 | 1767

BRAIN
A JOURNAL OF NEUROLOGY

Inflammatory myopathies associated with anti-mitochondrial antibodies

Meiko Hashimoto Maeda, Shoji Tsuji and Jun Shimizu

Department of Neurology, University of Tokyo, Graduate School of Medicine, 7-3-1 Hongo, Bunkyo-Ku, Tokyo 113-8655, Japan

Correspondence to: Jun Shimizu, MD, PhD,
Department of Neurology,
University of Tokyo,
Graduate School of Medicine, 7-3-1 Hongo,
Bunkyo-Ku, Tokyo 113-8655,
Japan
E-mail: jshimizu-tky@umin.net

Anti-mitochondrial antibodies, the characteristic markers of primary biliary cirrhosis, have been detected in most patients with this disease. However, the prevalence of these antibodies in inflammatory myopathies and their clinical and histopathological significance has not been determined. Sera from 212 consecutive patients with inflammatory myopathies were screened for anti-mitochondrial antibodies by enzyme-linked immunosorbent assay. The clinical and histopathological features of anti-mitochondrial antibody-positive patients were analysed and statistically compared with those of anti-mitochondrial antibody-negative patients. Twenty-four patients positive for anti-mitochondrial antibodies (seven patients with and 17 patients without primary biliary cirrhosis) were identified (11.3%). Thirteen patients had a clinically chronic disease course of >12 months before their diagnosis at hospitals. Six of these 13 patients (four asymptomatic patients with increased creatine kinase levels and two patients with arrhythmia) had not been aware of muscle weakness, but all 13 patients had muscle atrophy at initial presentation. As complications, eight patients had cardiac involvement including arrhythmias (five patients with supraventricular tachycardia; two with ventricular tachycardia; and one patient with atrioventricular block), six patients had moderately decreased ejection fraction and six patients had decreased vital capacity, two of whom required respiratory support. Regarding muscle histopathological findings, in addition to inflammation, 13 patients had chronic myopathic changes and six had granulomatous lesions. Statistical analysis showed that the clinical features of a chronic disease course, cardiac involvement and muscle atrophy, and the histopathological features of chronic myopathic changes and granulomatous inflammation, were significantly more frequently observed in patients with anti-mitochondrial antibody-positive inflammatory myopathy than in patients who were negative for anti-mitochondrial antibodies. Except for cardiac involvement, which is more frequently observed in patients with primary biliary cirrhosis, no significant differences in clinical or histopathological features were found between patients with or without primary biliary cirrhosis. Our study revealed that inflammatory myopathies associated with anti-mitochondrial antibodies were frequently found in patients with the clinical features of a chronic disease course, muscle atrophy and cardiopulmonary involvement, and the characteristic histopathological feature of granulomatous inflammation. Our study suggests that inflammatory myopathies associated with anti-mitochondrial antibodies form a characteristic subgroup.

Keywords: inflammatory myopathy; anti-mitochondrial antibodies; primary biliary cirrhosis; cardiac involvement; granulomatous inflammation

Abbreviations: AMA = anti-mitochondrial antibody; BCOADC = branched-chain 2-oxo acid dehydrogenase; E2 = E2-subunit; OGDC = 2-oxo glutarate dehydrogenase; PBC = primary biliary cirrhosis; PDC = pyruvate dehydrogenase complex

Received October 25, 2011. Revised March 6, 2012. Accepted March 8, 2012. Advance Access publication May 4, 2012

Introduction

Inflammatory myopathies are a heterogeneous group of autoimmune diseases characterized by progressive muscle weakness and skeletal muscle inflammation. Among them, cases of inflammatory myopathy associated with serum autoantibodies exhibit characteristic clinical features (Love *et al.*, 1991) in accordance with the type of autoantibody. Due to the close association between autoantibodies and characteristic clinical features, these autoantibodies are thought to be important not only as markers of subgroups of inflammatory myopathies, but also as factors involved in the mechanism underlying their pathogenesis (Love *et al.*, 1991; Greenberg and Amato, 2004).

Primary biliary cirrhosis (PBC) is a chronic inflammatory autoimmune disease that mainly targets the cholangiocytes of interlobular bile ducts in the liver. Histopathologically, the hallmark of the disease is a loss of biliary epithelial cells and small intrahepatic bile ducts with the portal infiltration of T cells, B cells, macrophages, eosinophils and natural killer cells (Hohenester *et al.*, 2009). The serological hallmark of the disease is the presence of circulating anti-mitochondrial antibodies (AMAs), which are found in 95% of cases with PBC (Van de Water *et al.*, 1988, 1989; Mutimer *et al.*, 1989; Miyakawa *et al.*, 2001). They act against members of the 2-oxoacid dehydrogenase complexes existing in the inner membrane of mitochondria. Among them, the major autoantigen is the E2-subunit of the pyruvate dehydrogenase complex (PDC-E2). The reactivity of AMAs against other 2-oxoacid dehydrogenase complexes, namely, 2-oxo glutarate dehydrogenase (OGDC-E2) and the branched-chain 2-oxo acid dehydrogenase (BCOADC-E2) is also found at a low frequency (Selmi *et al.*, 2011).

It has been reported that AMAs have a specificity of 98% for PBC when analysed with healthy controls (van de Water *et al.*, 1989); however, there are several case reports showing the associations of PBC or AMA positivity with other autoimmune diseases including systemic sclerosis, Sjögren's syndrome, rheumatoid arthritis (Manthorpe *et al.*, 1979; Berg *et al.*, 1986; Skopouli *et al.*, 1994) and sensory ataxic neuropathy (Charron *et al.*, 1980; Illa *et al.*, 1989; Dahlan *et al.*, 2003; Talwalkar and Lindor, 2003). Thus, the prevalence and the significance of AMAs in autoimmune disease have not yet been studied systematically.

When it comes to the association of PBC with inflammatory myopathies, there have been 23 case reports (Uhl *et al.*, 1974; Benoist *et al.*, 1977; Epstein *et al.*, 1981; Willson, 1981; Tsuchiya *et al.*, 1985; Kumazawa *et al.*, 1987; Saitoh *et al.*, 1988; Ueda *et al.*, 1988; Milosevic and Adams, 1990; Yasuda *et al.*, 1990; Mader *et al.*, 1991; Harada *et al.*, 1992; Varga *et al.*, 1993; Boki and Dourakis, 1995; Simpson and Nickl, 1995; Nakasho *et al.*, 1996; Ono *et al.*, 1996; Tsai *et al.*, 1996; Matsui *et al.*, 2000; Kasuga *et al.*, 2004; Tanaka *et al.*, 2007; Honma *et al.*, 2008), since the first report by Uhl *et al.* (1974). In these case reports, clinical features including a chronic progressive course (Tsuchiya *et al.*, 1985; Milosevic and Adams, 1990; Harada *et al.*, 1992; Matsui *et al.*, 2000; Kasuga *et al.*, 2004; Tanaka *et al.*, 2007), cardiac involvement (Uhl *et al.*, 1974; Saitoh *et al.*, 1988; Harada *et al.*, 1992; Varga *et al.*, 1993; Tsai *et al.*, 1996; Kasuga *et al.*, 2004; Tanaka *et al.*, 2007), respiratory muscle weakness (Varga *et al.*, 1993; Matsui *et al.*, 2000; Kasuga *et al.*, 2004; Tanaka *et al.*, 2007) and muscle atrophy (Tsuchiya *et al.*, 1985; Kumazawa *et al.*, 1987; Saitoh *et al.*, 1988; Ueda *et al.*, 1988; Varga *et al.*, 1993; Tsai *et al.*, 1996) were described. Although previous reports suggest some characteristic clinical features of inflammatory myopathies associated with PBC, because of the lack of large-scale and systemic clinical and histopathological studies, the prevalence of PBC in inflammatory myopathies is unknown, and the characteristic clinical and histopathological features of inflammatory myopathy-associated PBC have not yet been clarified.

In this study, we retrospectively reviewed 212 patients with inflammatory myopathies and found 24 patients with AMA-positive myositis (11.3%) (seven patients with and 17 patients without PBC). The analysis of clinical and histopathological features revealed that inflammatory myopathies associated with AMAs frequently include patients with a clinically chronic disease course, muscle atrophy, cardiopulmonary involvement and granulomatous inflammation, regardless of the presence or absence of PBC. Our study suggests that inflammatory myopathies associated with AMAs form a characteristic subgroup.

Patients and methods

For the screening of patients with AMA-positive myositis, 212 consecutive patients with inflammatory myopathies referred to our department between November 1999 and April 2009 and whose serum samples were available were included in this study. The diagnosis of inflammatory myopathy was based on the criteria proposed by Bohan and Peter (1975*a*, *b*); in addition, one or two muscle biopsy findings, namely, inflammatory changes with necrotic and/or regenerating fibres and major histocompatibility complex (MHC) class I expression on non-necrotic muscle fibres (Bohan and Peter, 1975*a*, *b*; Hoogendijk *et al.*, 2004) and exclusion of muscular dystrophy by immunohistochemistry were required. For the exclusion of inclusion body myositis, the criteria proposed by Griggs *et al.* (1995) were used, and sarcoid myopathy was excluded on the basis of clinical data including roentgen findings of the chest (Iannuzzi *et al.*, 2007) and the titre of the angiotensin I-converting enzyme in serum.

The clinical records of the patients were reviewed to obtain clinical information. The clinical criteria established by the American Association for the Study of Liver Diseases (Lindor *et al.*, 2009) were used for the diagnosis of PBC. The disease duration before diagnosis was defined as the duration between the time of the initial awareness of the symptoms and the time of muscle biopsy for histopathological diagnosis. In the assessment of neurological or laboratory studies, the findings at the time of muscle biopsy were used. Muscle power was evaluated using the Medical Research Council scale.

For the detection of AMAs, serum samples taken before the initiation of therapy and stored at −80°C were used. AMA titre was determined by enzyme-linked immunosorbent assay using a MESACUP-2 Test Mitochondria M2 (AMA-M2) kit (Medical and Biological Laboratories) (Kadokawa *et al.*, 2003). In this method, recombinant PDC-E2, BCOADC-E2 and OGDC-E2 antigens are used as coating antigens, and peroxidase-conjugated anti-human immunoglobulin polyclonal antibody is used as a conjugate antibody to enable the capture the immunoglobulin G, M and A class autoantibodies against AMAs. Briefly, 100 µl of a patient's diluted serum was

added to each well of a microtitre plate precoated with recombinant PDC-E2, BCOADC-E2 and OGDC-E2 antigens, and incubated at room temperature for 60 min to allow anti-PDC-E2, -BCOADC-E2 and -OGDC-E2 antibodies to react with immobilized antigens. After washing, a peroxidase-conjugated goat anti-human immunoglobulin polyclonal antibody was dispensed into each well of the plate and incubated at room temperature for 60 min. Following another washing step, a peroxidase substrate was mixed with a chromogen and incubated at room temperature for 30 min. An acid solution (H_2SO_4) was then added to each well to terminate the enzyme reaction. The colour development was measured in a microplate reader at a frequency of 450 nm. 'Calibrator 1' (serum of 0 index) and 'Calibrator 2' (serum of 100 index) were also tested similarly. The index value was calculated using the following formula: (absorbance value of test serum – absorbance value of Calibrator 1)/(absorbance value of Calibrator 2 – absorbance value of Calibrator 1) × 100. Using this method, an index value of >7, which was determined using 168 normal control serum samples, was considered to indicate positivity for the antigens of interest with 90% sensitivity and 98% specificity (Takemura *et al.*, 2001; Kadokawa *et al.*, 2003). Myositis-specific/related autoantibodies including anti-Jo-1, -SRP, -Mi-2, -PL-7 and -PM/Scl100 antibodies were detected by the dot-blot method using recombinant Jo-1, SRP, Mi-2, PL-7 and PM/Scl100 (Diarect AG).

In all cases, biopsied muscle samples were processed for routine histochemistry and immunohistochemistry for the MHC class I, MHC class II, CD4, CD8, CD45, CD68 and C5b-9 antigens (DAKO).

During the analysis of clinical and histopathological features, differences between AMA-positive and -negative patients with myositis were compared. The differences were also analysed between AMA-positive myositis patients with PBC and those without PBC.

For the analysis of the correlation between the index AMA titre and clinical features (disease duration before diagnosis, modified Rankin scale and Medical Research Council scale), a simple linear regression was carried out. A two-tailed Mann–Whitney test was performed for different sets of continuous data of clinical features and a Fisher's exact test was used to compare categorical data. A *P*-value of <0.05 was considered significant.

Results

Patients with inflammatory myopathy and anti-mitochondrial antibodies

Twenty-four patients with AMA-positive myositis were identified among 212 consecutive patients with inflammatory myopathies referred to our department. Thus, the prevalence of AMAs in myositis was 11.3%. The clinical and histopathological findings of AMA-positive patients are shown in Table 1. Of the 24 patients, seven, including two with liver histopathological findings consistent with PBC, showed biochemical evidence of cholestasis with an increased alkaline phosphatase level and fulfilled the diagnostic criteria (Lindor *et al.*, 2009) of PBC. Thus, these seven patients were diagnosed as having myositis with PBC and 17 patients were diagnosed as having myositis-associated AMAs without any clinical features of PBC. In the seven patients with PBC, PBC preceded the development of inflammatory myopathies in three patients, whereas PBC and inflammatory myopathies were diagnosed concurrently in four patients. With regard to coexisting diseases other than PBC, seven patients had inflammatory myopathies associated with collagen diseases: (i) two patients with PBC: Sjögren's syndrome and systemic sclerosis, $n = 1$; ulcerative colitis, $n = 1$; (ii) 5 of 17 patients without PBC: systemic sclerosis, $n = 2$; systemic lupus erythematosus, $n = 2$; rheumatoid arthritis, $n = 1$; and (iii) three patients had inflammatory myopathies associated with malignancies: colon cancer, $n = 1$; tongue cancer, $n = 1$; stomach and colon cancer, $n = 1$, two within 1 year of admission and one concurrently.

Of the 24 myositis patients with AMA, nine were male and 15 were female. The average age at disease onset was 54 years (range 32–86 years).The average disease duration before diagnosis was 20 months (range 1–60 months) and the disease duration was >12 months in 13 patients (six patients with PBC and seven patients without PBC). The initial symptoms of the 24 patients were muscle weakness or atrophy in 18 patients, arrhythmia in two patients, and no subjective muscle symptoms except for an increased serum creatine kinase level found by chance during medical checkups in four patients.

Regarding neurological findings, all 24 patients, except for one with diffuse muscle weakness (Patient 17), showed muscle weakness with proximal dominance. Thirteen patients showed muscle atrophy (four patients with PBC and nine patients without PBC) and three patients with 24 or 60 months of disease duration showed lordotic posture (Patients 5, 7 and 23). Regarding laboratory findings, serum creatine kinase levels were elevated in all patients ranging from 232 to 15132 IU/l (2322 ± 3121 I/U).

The associated autoantibodies were detected in 10 of 24 patients with myositis with AMAs: (i) in six of seven patients with PBC: anti-nuclear antibody, $n = 4$; rheumatoid factor, $n = 3$; anti-Sjögren's syndrome-A antibody, $n = 2$; anti-Sjögren's syndrome-B antibody, $n = 1$; (ii) in 14 of 17 patients without PBC: anti-nuclear antibody, $n = 12$; rheumatoid factor, $n = 7$; anti-Sjögren's syndrome-A antibody, $n = 1$; anti-Sjögren's syndrome-B antibody, $n = 1$.

Muscle CT images were assessed in 13 patients, and 10 patients showed muscle atrophy with proximal dominance, and three patients (Patients 5, 7 and 23) with lordotic posture showed atrophy with fatty changes in paravertebral muscles (Fig. 1).

Regarding cardiac involvements, eight patients (five patients with PBC and three patients without PBC) showed arrhythmias (supraventricular tachycardia, $n = 5$; ventricular tachycardia, $n = 2$; atrioventricular block, $n = 1$), and six patients (four patients with PBC and two patients without PBC) showed a decreased ejection fraction (<50%). In the patients with arrhythmias, two (Patients 7 and 23) were treated by catheter ablation. With regard to respiratory involvements, six patients (two patients with PBC and four patients without PBC) had a vital capacity of <80%. Among them, two patients (Patients 3 and 7) required respiratory support.

Detailed information about the responses to treatments was available in 15 patients (observation period, 35.0 ± 34.8 months; range 3–96 months). Among them, 11 patients were treated with corticosteroids, one patient was treated with azathioprine and three patients refused treatment. In our series, bile acid therapy had been performed in only one patient (Patient 1, three years before the diagnosis of myositis). Thus, it was difficult to know

Table 1 Baseline characteristics and treatment response for individual subjects

Patient No.	1	2	3	4	5	6	7	8	9	10	11	12	13	14	15	16	17	18	19	20	21	22	23	24
Onset age (years)/sex	54/F	72/F	49/F	48/M	54/F	39/F	59/M	67/F	68/M	39/M	44/F	33/F	34/F	86/M	65/F	58/F	67/F	57/M	64/F	57/M	46/F	53/M	54/M	32/F
Disease duration before diagnosis (months)	11	12	24	24	24	24	60	1	1	2	2.5	3	3	5	6	6	10	12	17	24	36	48	60	60
Initial symptoms	Mu	C	Mu	Mu	A	Mu	Mu	C	Mu	C	Mu	Mu	Mu	Mu	Mu	C	Mu	Mu	Mu	Mu	Mu	Mu	A	Mu
Clinical signs and symptoms																								
Weakness (MRC)																								
Neck (flexion)	NE	3	4	3	4	4	4	4	5	5	4	3	4	5	3	3	NE	5	4	5	3	4	2	5
UE (proximal/distal)	4/5	4/5	4/5	3/5	4/5	4/5	3/4	5/5	4/5	4/5	3/4	4/4	4/4	5/5	4/4	4/5	3/3	3/4	5/5	5/5	4/5	3/5	4/4	5/5
LE (proximal/distal)	5/5	4/5	4/5	4/5	4/5	4/5	3/3	4/5	4/5	4/5	3/4	4/5	4/5	4/5	3/4	5/5	3/3	4/5	4/5	4/5	4/5	4/4	4/5	4/5
Muscle atrophy	(−)	(−)	(+)	(+)	(+)	NE	(+)	NE	NE	NE	NE	(+)	(+)	NE	(+)	NE	NE	(+)	(+)	NE	(+)	(+)	(+)	(+)
Lordotic posture	(−)	(−)	(−)	(−)	(+)	(−)	(+)	(−)	(−)	(−)	(−)	(−)	(−)	(−)	(−)	(−)	(−)	(−)	(−)	(−)	(−)	(−)	(+)	(−)
Arrhythmia	AF	(−)	Af, PSVT	AV block	NSVT (PM)	(−)	AF (CA)	(−)	(−)	(−)	(−)	(−)	(−)	(−)	(−)	Paf	(−)	(−)	(−)	(−)	Af	(−)	CRBBB, PVC (CA)	(−)
Cardiomyopathies[a]	(+)	(−)	(−)	(+)	(+)	(−)	(+)	(−)	(−)	(−)	(−)	(−)	(−)	(−)	(−)	(+)	(−)	(−)	(−)	(−)	(−)	(−)	(+)	(−)
Restrictive ventilatory impairment (vital capacity)	(−)	(−)	(+); NIPPV	(−)	(−)	(−)	(+) (45.8%); NIPPV	NE	(−)	NE	NE	(−)	(−)	NE	(−)	(+) (50.0%)	(+) (68.9%)	NE	(−)	(−)	(−)	(+) (56.0%)	(+) (77.5%)	NE
Modified Rankin scale	1	1	2	2	1	2	3	1	1	1	1	1	1	1	2	2	3	2	3	1	1	2	2	1
PBC preceding (duration: months)	(+) 84	(−)	(−)	(−)	(+) 84	(+) 10	(−)	(−)	(−)	(−)	(−)	(−)	(−)	(−)	(−)	(−)	(−)	(−)	(−)	(−)	(−)	(−)	(−)	(−)
Diagnosis type of PBC	Asymp.	Asymp.	Asymp.	Asymp.	Asymp.	Symp.	Asymp.	(−)	(−)	(−)	(−)	(−)	(−)	(−)	(−)	(−)	(−)	(−)	(−)	(−)	(−)	(−)	(−)	(−)
Associated disorders																								
Collagen disease	Ulcerative colitis	SS, SSc	(−)	(−)	(−)	(−)	(−)	(−)	(−)	(−)	(−)	(−)	(−)	(−)	(−)	SSc	SLE	SLE	SSc	(−)	(−)	RA	(−)	(−)
Malignant disease	(−)	(−)	(−)	(−)	(−)	(−)	(−)	(−)	Colon Ca	(−)	Tongue Ca	(−)	(−)	Stomach Ca, Colon Ca	(−)	(−)	(−)	(−)	(−)	(−)	(−)	(−)	(−)	(−)
Laboratory data																								
CK level (IU/l)	1085	533	488	3620	619	1381	558	232	4230	15132	4000	1770	4332	692	1170	569	5147	1143	258	1844	2398	280	924	3325
ESR (mm/h)	96	49	104	81	36	71	NE	22	61	NE	42	33	22	34	23	67	83	39	19	61	38	68	NE	29
CRP level (mg/dl)	0.5	0.2	1	0.5	0.49	0.9	1.4	1.6	2.7	2.6	2.3	0.3	0	0.6	0.05	0.9	0	1.43	0.06	0.3	<0.3	0.43	0.26	0
ALP level(U/l)[b]	1540*	292*	754*	515*	381*	850*	309*	192*	135*	151*	NE	NE	220*	NE	253*	36*	NE	NE	122**	NE	153*	127*	179**	NE
AMAs (index)	95.5	100.3	114	117.9	119.5	25	116.2	15.8	7.4	37.6	18.1	90.8	13.4	109.4	36.7	8.6	12.8	20	67.6	124.3	57.8	27.9	85.1	85.3
Anti-nuclear antibodies		X1280 (sp)	RNP		X40 (sp)	X160 (sp)		X40 (sp, homo)	dsDNA			X80 (spe)	X5120 (sp, nucl), RNP	X40 (sp)		X2560 (sp), Scl70	dsDNA, RNP	X5120 (sp), Scl70, RNP	X320 (sp, nucl)	centromere		X320 (sp, nucl), dsDNA		dsDNA
Other autoantibodies		SS-A, SS-B		RF		RF	SS-A, RF		RF	RF	RF						SS-A, SS-B, RF	RF				RF		RF
Myositis-specific/related autoantibodies	(−)	(−)	(−)	(−)	(−)	(−)	(−)	(−)	(−)	Jo-1	(−)	(−)	(−)	(−)	(−)	(−)	(−)	(−)	(−)	(−)	(−)	(−)	(−)	(−)
Liver biopsy	CNSDC	NE	NE	CNSDC	NE	NE	NE	NE	NE	NE	NE	NE	NE	NE	NE	NE	NE	NE	NE	NE	NE	NE	NE	NE
Treatment response																								
Treatment	(−)	(−)	NI	CS	(−)	NI	AZP	NI	CS	CS	CS	CS	NI	NI	CS	CS	NI	NI	CS	NI	CS	CS	CS	NI
Follow-up period (months)	96	36	NI	84	54	NI	12	NI	12	3	3	12	NI	NI	6	90	NI	NI	36	NI	84	12	12	NI
Modified Rankin scale change	1→1	1→1	NI	2→0	1→1	NI	3→2	NI	1→0	1→1	1→0	1→0	NI	NI	2→2	2→2	NI	NI	3→1	NI	1→1	2→2	2→2	NI
Worsening of arrhythmia	(+)	(−)	NI	(+)	(+)	NI	(−)	NI	(−)	(−)	(−)	(−)	NI	NI	(−)	(−)	NI	NI	(−)	NI	(−)	(−)	(−)	NI
CK level (IU/l) after treatment	NE	w.n.l.	NI	w.n.l.	w.n.l.	NI	w.n.l.	NI	w.n.l.	w.n.l.	w.n.l.	w.n.l.	NI	NI	w.n.l.	w.n.l.	NI	NI	w.n.l.	NI	934	w.n.l.	w.n.l.	NI

(continued)